

Synchrotron Imaging

Sheridan Mayo

30 May 2017

CSIRO MANUFACTURING
www.csiro.au



X-ray imaging – a long history



A print of one of the first X-rays by Wilhelm Röntgen (1845–1923) of the left hand of his wife Anna Bertha Ludwig (taken 22 Dec 1895)

- Wilhelm Röntgen took first x-ray image in 1895.
- X-rays used in medical imaging from 1896 onwards
- First sources of x-rays were x-ray tubes: polychromatic, relatively low-power x-ray sources.
- Synchrotron imaging opened up a range of new imaging possibilities

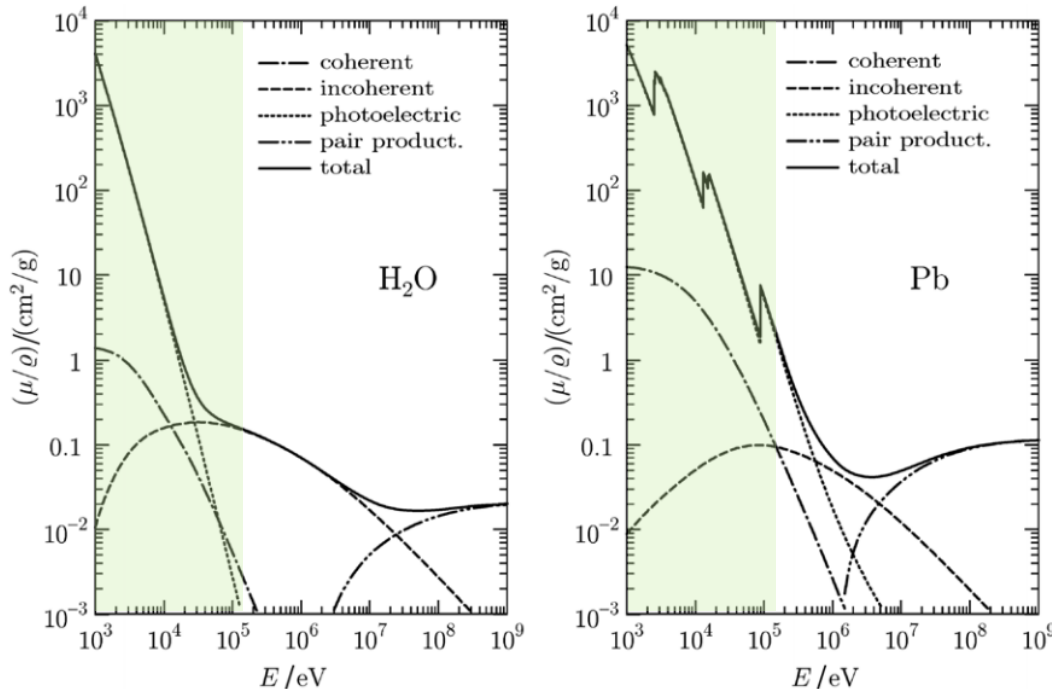


X-ray imaging basics – beam attenuation

Multiple processes can attenuate the x-ray beam passing through the sample.

For typical x-ray energies used at synchrotrons the photoelectric effect dominates for many materials, but for low Z materials incoherent scattering becomes more important at higher energies >20keV.

Shown below are total mass attenuation curves for water and lead (dotted lines show contributions from different mechanisms). The areas in green show energy range accessible at synchrotron sources.

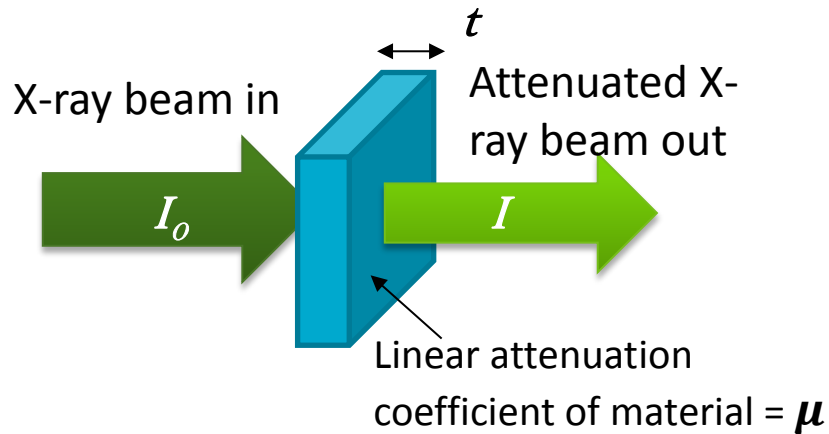


Salvat et al, Metrologia 46 (2009) S112–S138

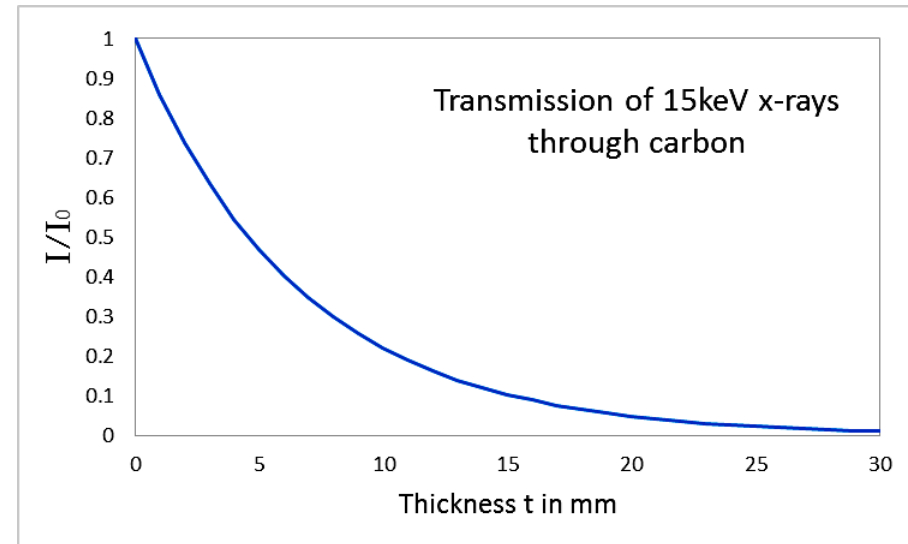
- Photoelectric effect is the complete absorption of the x-ray photon by an atom resulting in the ejection of an electron.
- Incoherent scattering causes the x-ray photon to lose some but not all of its energy in being scattered from the atom.
- Linear attenuation coefficient μ_{lin} is calculated by multiplying mass attenuation coefficient, μ_{mass} by material density ρ

$$\mu_{lin} = \rho \mu_{mass}$$

X-ray imaging basics – Beer's law



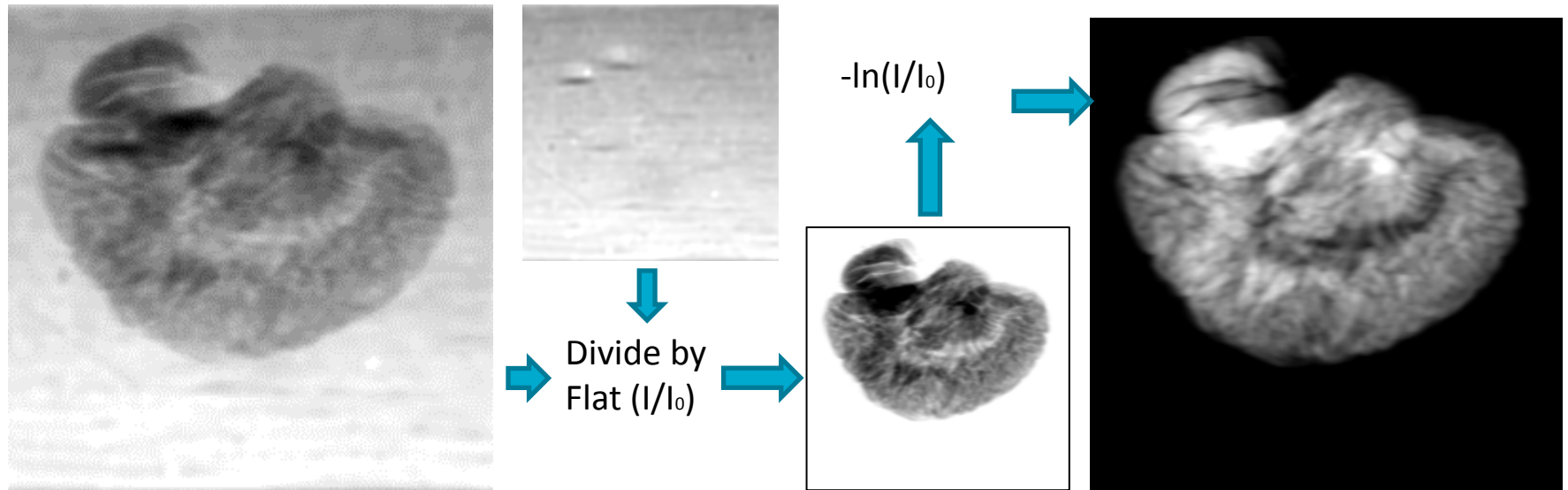
$$I = I_0 e^{-\mu t}$$



- X-ray absorption by an object depends on the x-ray energy, and the thickness t and linear x-ray attenuation coefficient μ of the materials the x-rays are passing through. For a monochromatic beam passing through a homogenous material the x-ray intensity reduces exponentially with distance. This is known as **Beer's law**.
- Linear attenuation coefficient indicates how strongly a material absorbs x-rays. It depends on x-ray energy and the elemental composition and density of the material. It can be calculated from the mass attenuation coefficient times density.

X-ray imaging basics: Beers law

For a composite object imaged with a monochromatic beam Beer's law is written as the integral of $\mu(t)$ with respect to t in the beam direction. For a monochromatic beam this is shown below:

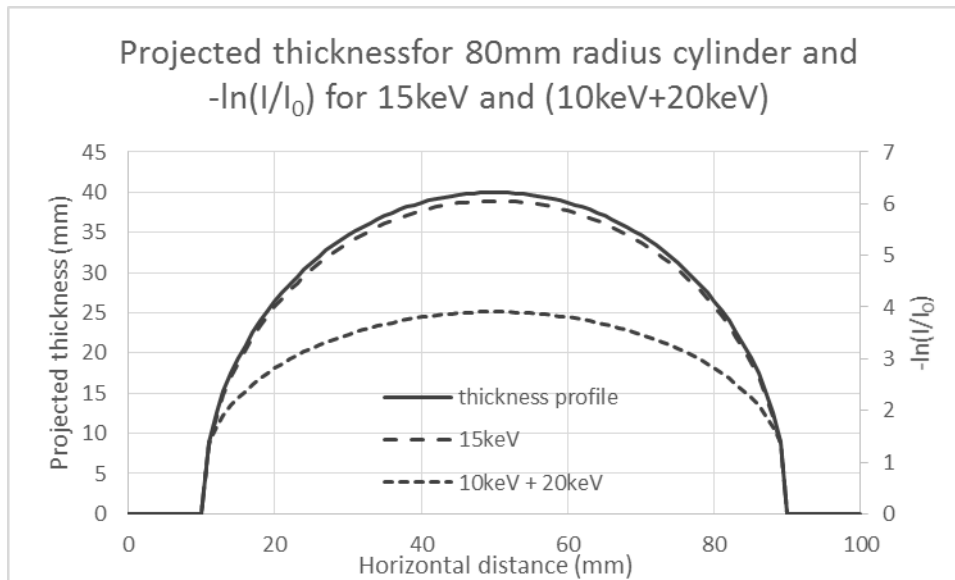
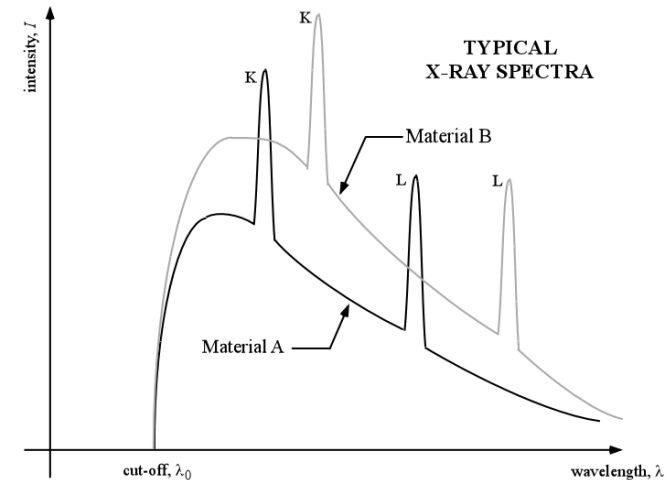


$$I = I_0 e^{-\mu t}$$

$$\mu t = -\ln\left(\frac{I}{I_0}\right)$$

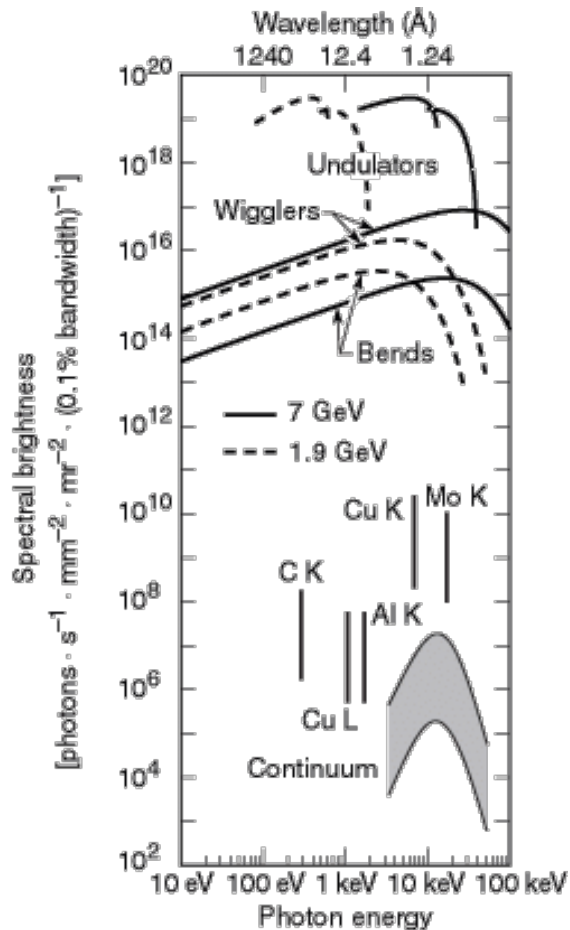
X-ray imaging basics: Beam hardening

For laboratory sources beam is polychromatic and beam hardening is an issue. There is no longer simple Beer's law relationship between x-ray absorption and thickness and thickest part of the object appear less absorbing that you would expect compared to thinner parts as the spectrum passing through this part is on the whole harder (higher energy) and more penetrating.



Shown left is a comparison between $-\ln(I/I_0)$ for monochromatic 15keV beam and polychromatic beam (10keV+20keV) of average energy 15keV. For the monochromatic beam the $-\ln(I/I_0)$ curve is the same shape as the thickness profile, but by comparison the dual energy curve is flattened at the top as it is less absorbing in the thicker part by comparison. This is because very little of the 10keV x-rays contribute to this part of the image.

Why synchrotron imaging?



Source: X-ray data booklet ('little orange book') <http://xdb.lbl.gov/>

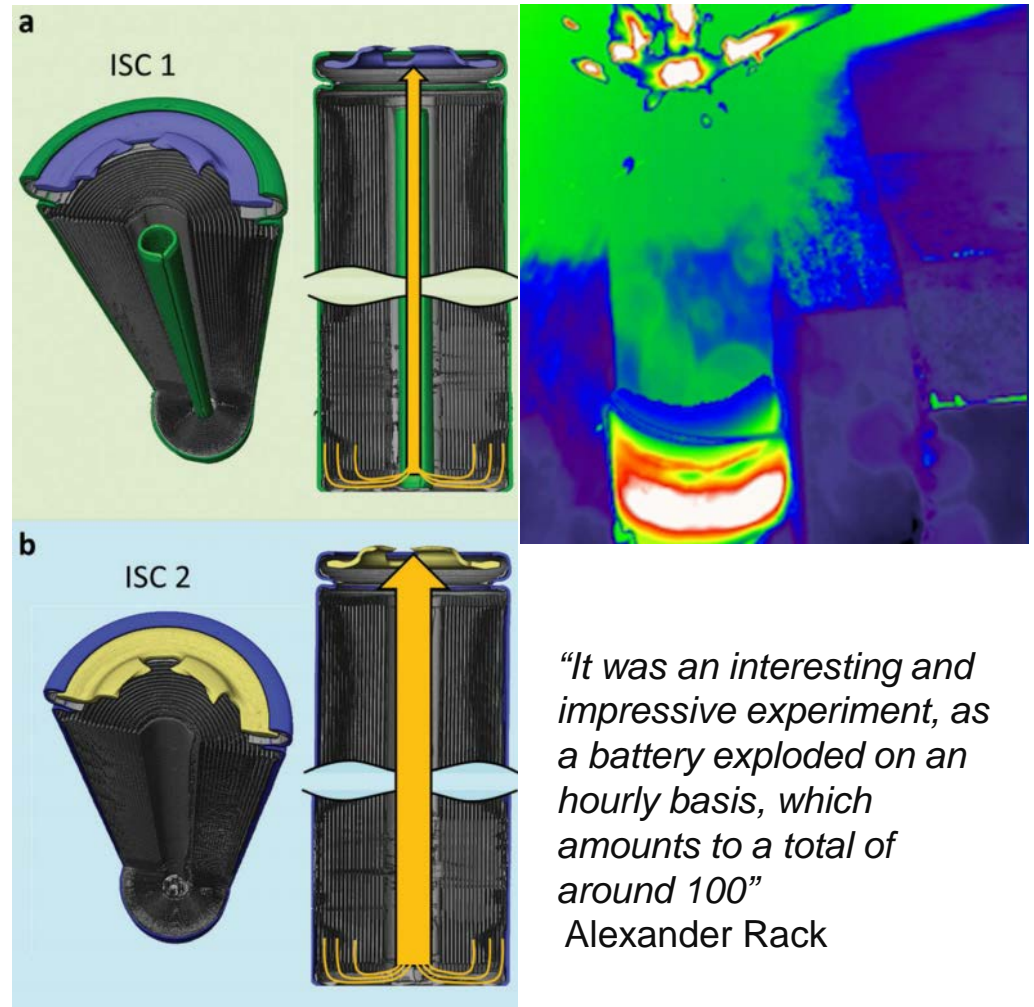
- Intensity and brightness – much higher speed, better signal to noise, rapid tomography
- Monochromatic and tunable beam – no beam-hardening artefacts, beam energy tailored to experiment, K-edge subtraction
- High coherence – phase contrast imaging modes such as inline, analyser-based, grating-based
- Specialised beams – polarisation, pulsed beam (from single bunch mode)

High-speed imaging – exploding batteries!

Finegan et al, Energy Environ. Sci., 2017

Lithium ion batteries are widely used in laptops, phones and other portable devices. However they have been known to explode making safety a concern. This experiment deliberately short-circuited over 100 x 18 640 Li-ion cells and observed the results with high-speed synchrotron imaging

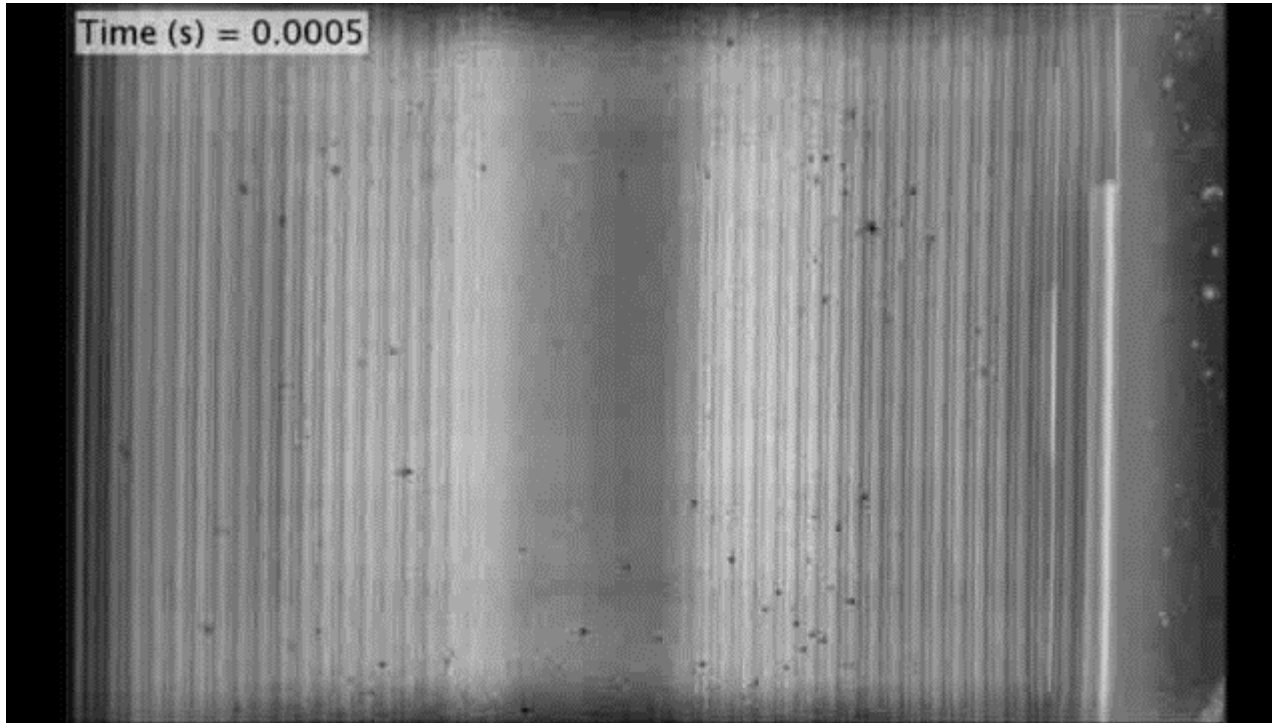
In the event of failure the sealed shell can act as a dangerous pressure vessel. Two types of cell designs were compared. The ISC 1 had a mandrel intended to allow gas to escape in the event of failure and reduce the risk of bursting.



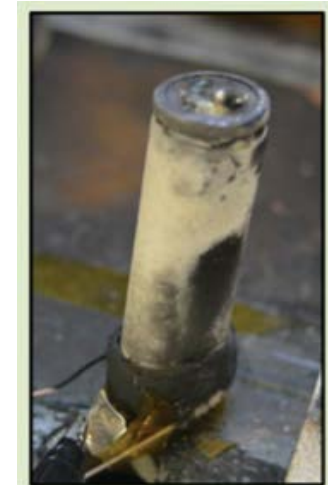
“It was an interesting and impressive experiment, as a battery exploded on an hourly basis, which amounts to a total of around 100”

Alexander Rack

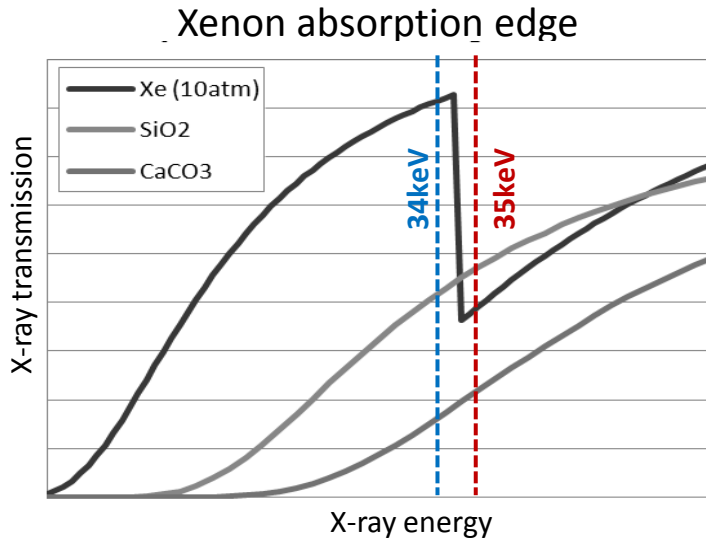
High-speed imaging – exploding batteries!



Finegan et al, Energy Environ. Sci., 2017



K-edge subtraction & contrast agents



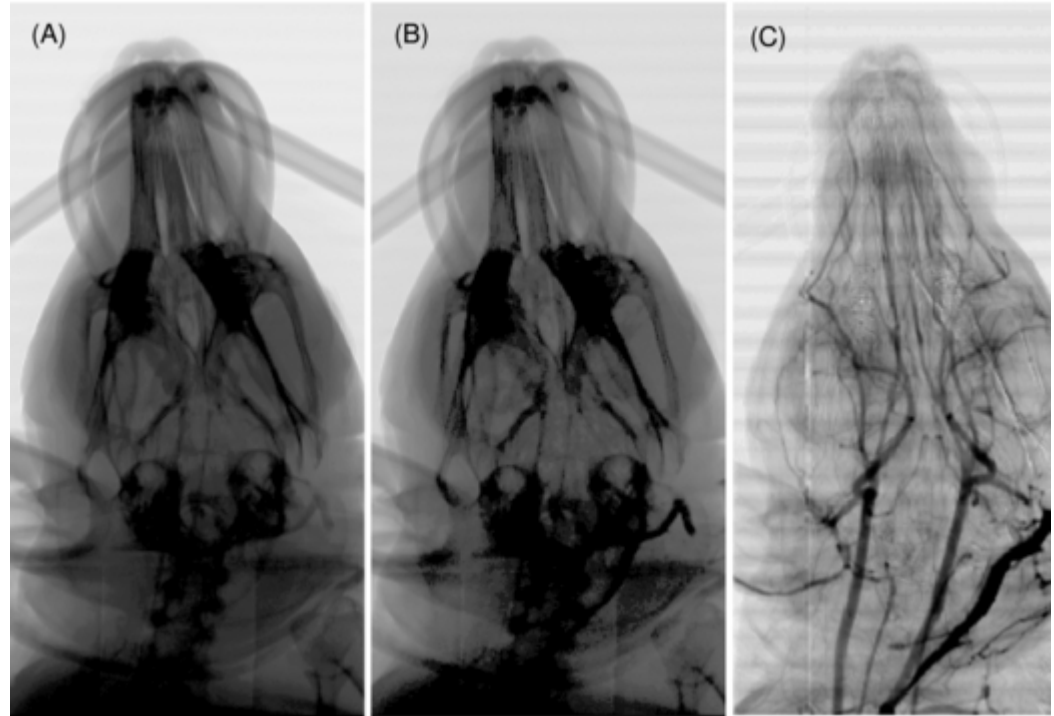
By subtracting the image taken below the absorption edge from that above, the contribution to the image from the contrast agent (or element of interest) is isolated. The x-ray attenuation of other materials does not change significantly between above and below the absorption edge

K-edge subtraction & contrast agents

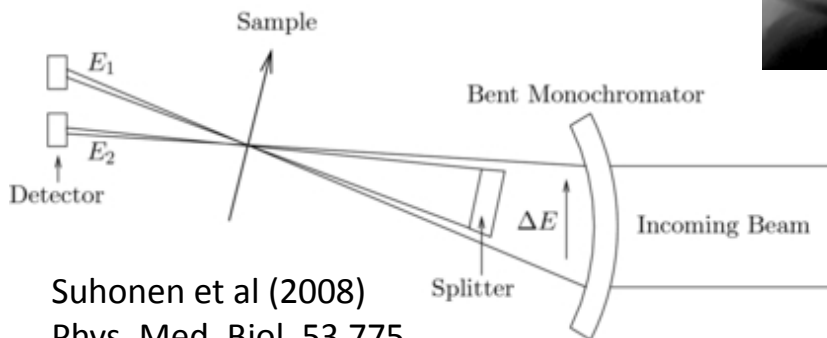
Kelly et al (2007) Phys. Med. Biol. 52 1001

K-edge digital subtraction angiography of rabbit using an iodine contrast agent made even smaller vessels visible.

Cerebral Bent Laue monochromators at ESRF's ID17 allows simultaneous acquisition of images above and below the iodine absorption edge at 33keV



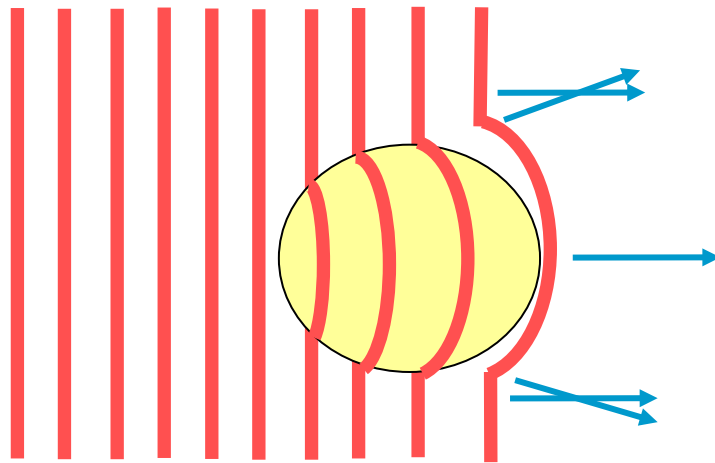
Images acquired below (A) and above (B) the K-edge of iodine, both without easily discernible contrast in the cerebral arteries. The subtracted image (C), however, shows very good contrast in the cerebral arteries.



Suhonen et al (2008)
Phys. Med. Biol. 53 775

Phase-contrast imaging – refraction of x-rays

X-rays are not only absorbed by an object, they can be refracted. The refractive index, n , consists of real and imaginary parts, δ and β . The imaginary part describes absorption and the real part refraction. For x-rays the real component of the refractive index for most media is **less than 1** so that the wavefront is advanced on passing through a materials relative to an undisturbed wavefront.



$$n = 1 - \delta - i\beta$$

$$\psi = 2\pi\delta/\lambda \quad \mu = 2\pi\beta/\lambda$$

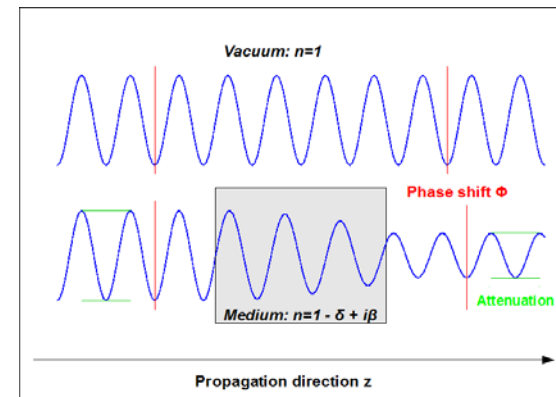
For homogenous medium of thickness t

Phase shift

$$\phi = \psi t$$

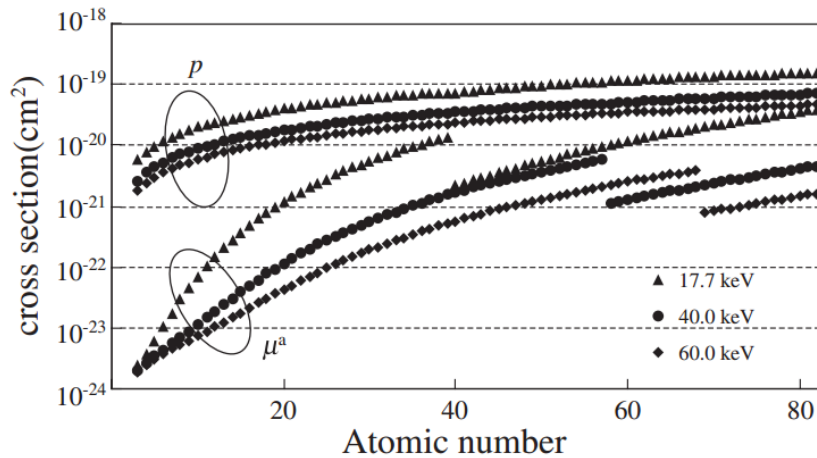
Attenuation

$$I/I_0 = e^{-\mu t}$$



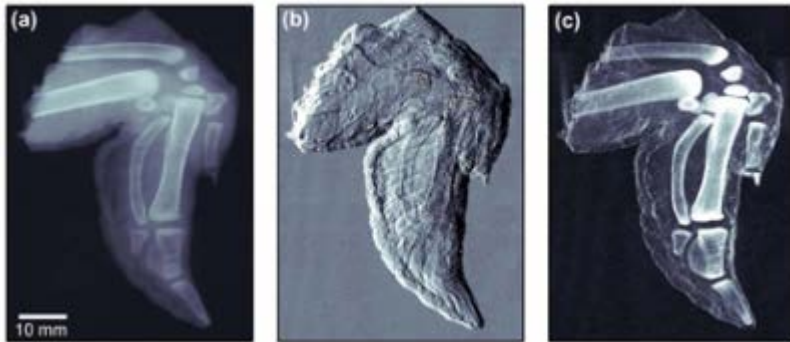
On passing through a typical object this results in a distortion of the wavefront and small changes in beam propagation direction.

Why is phase contrast valuable?

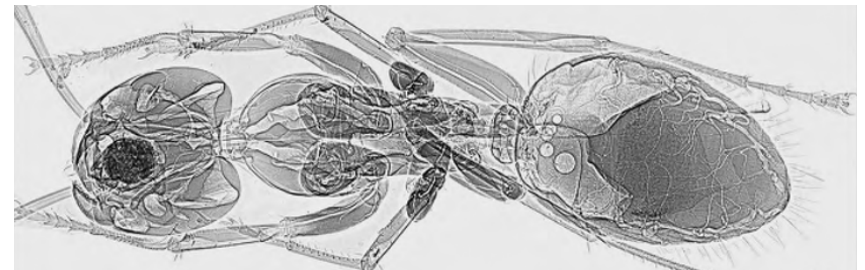


Interaction cross section of absorption μ_a and phase shift cross sections vs atomic number (Momose, Jpn. J. Appl. Phys., Vol. 44, No. 9A, 2005)

- For low-atomic number materials the phase-shift cross section is much larger than the absorption cross section.
- The phase-contrast mechanism enables us to see low-contrast 'soft' materials much more effectively than absorption contrast.
- It also makes it possible to visualise low-density materials in the presence of high x-ray absorbing materials such as soft tissue around bone.
- Phase contrast modes typically highlight the first or second derivative of the phase shift, highlighting edges and boundaries.



https://www.dectris.com/pci_application.html



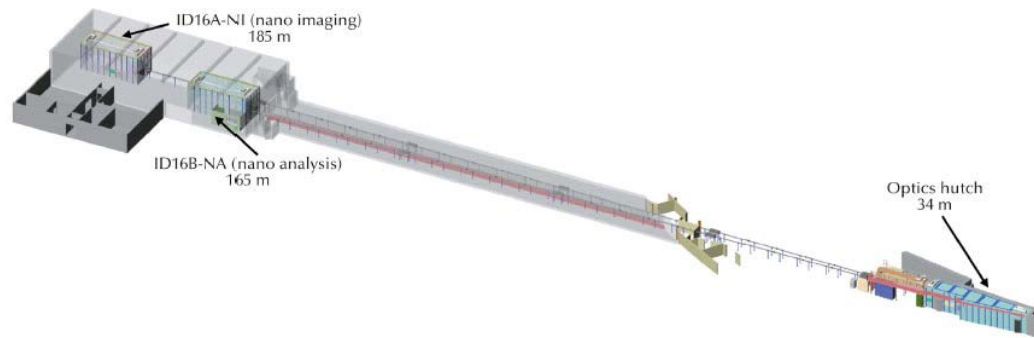
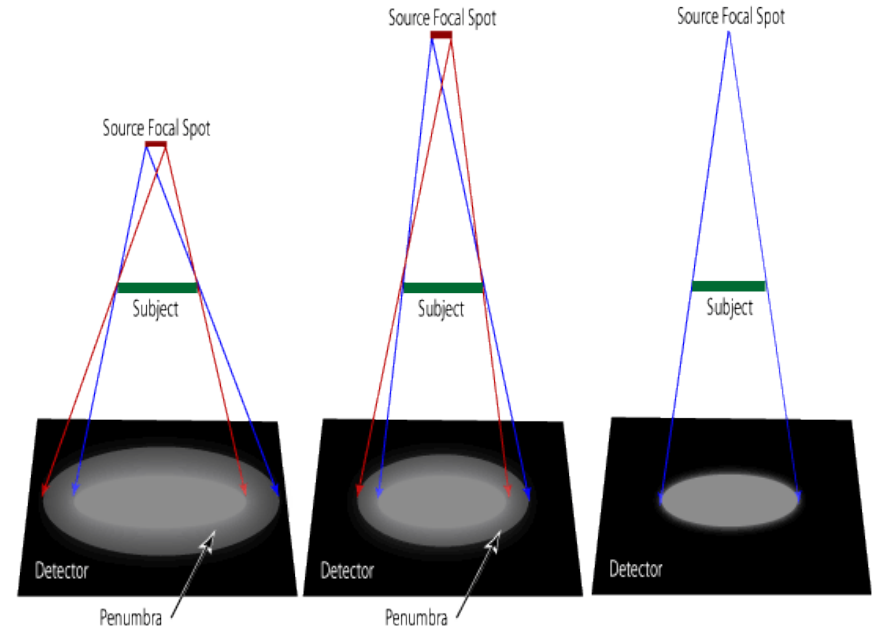
J.J. Socha et al. / Resp. Phys. & Neurobiol.173S (2010) S65–S73

Phase-contrast requirements

Successful phase-contrast imaging depends on the ability to detect small changes in direction of the transmitted x-ray beam. This is only possible if the incident x-ray is spatially coherent.

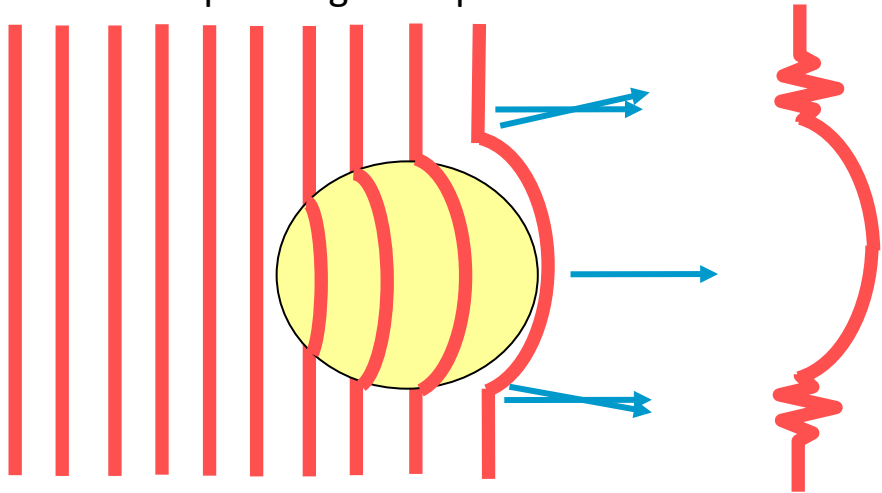
An incoherent source will cause the x-ray image to suffer from penumbral blurring when there is a space between the sample and the detector.

Spatial coherence can be achieved by having a source that is either small or far away.



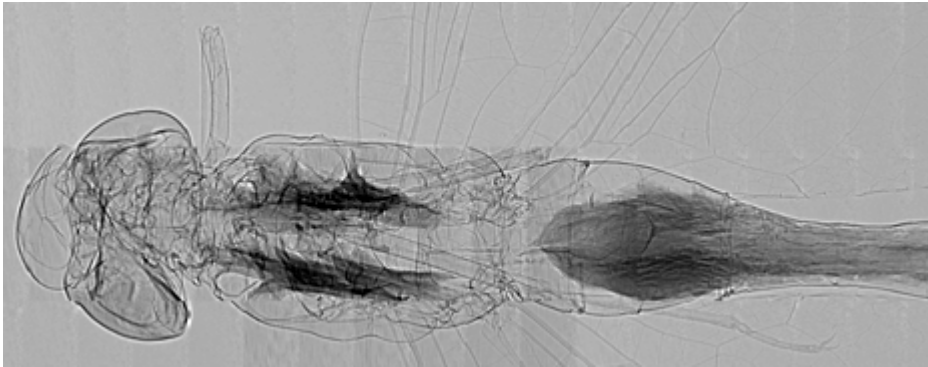
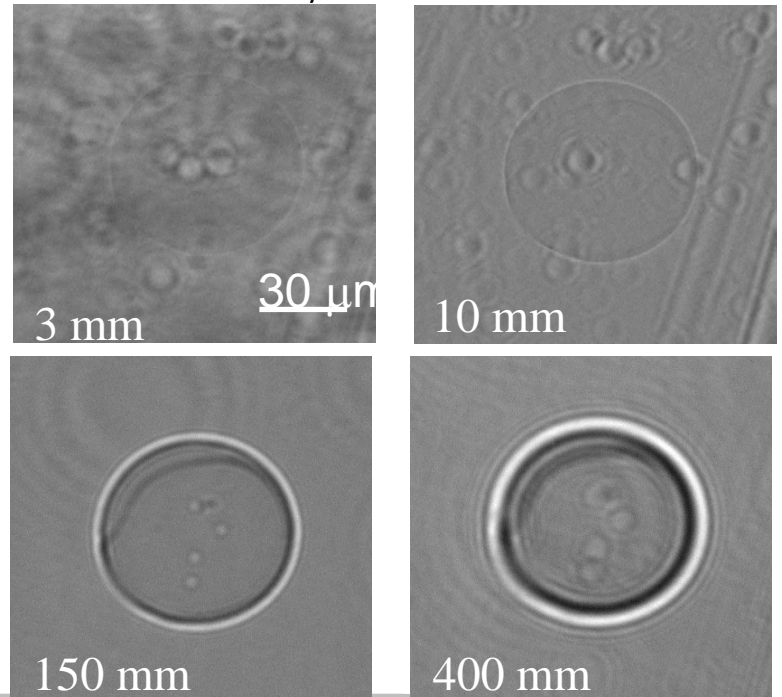
In-line phase-contrast imaging

This is the simplest form of phase-contrast imaging. Phase-contrast is achieved by increasing the gap between the sample and the detector. This allows rays which have been deflected by the sample to interfere. The resulting image shows near-field Fresnel diffraction, enhancing edges and boundaries but still incorporating absorption contrast.

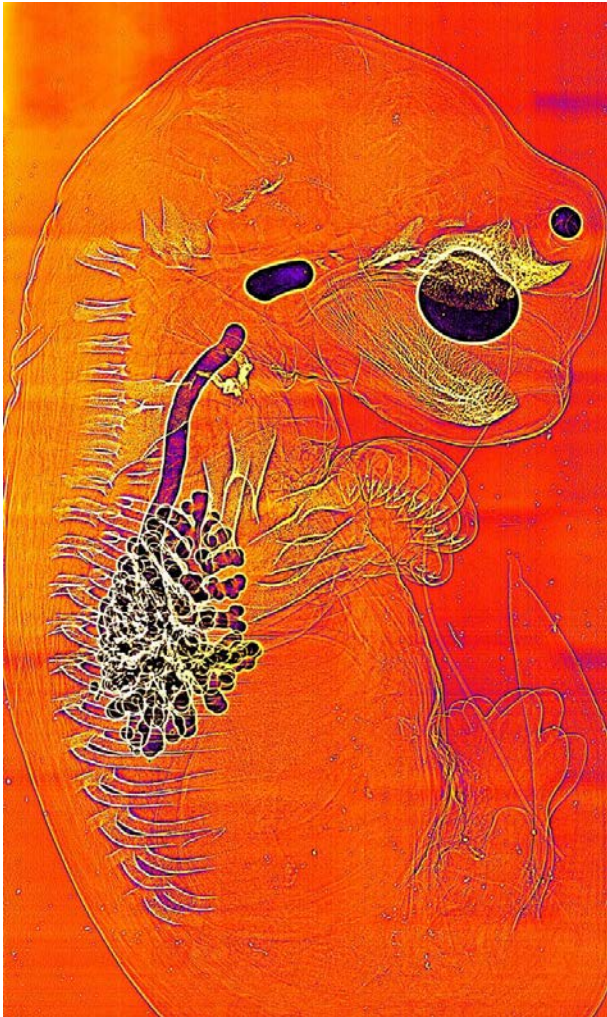


For a pure phase-object – near-field image is Laplacian of phase distribution $\nabla^2 \phi(x,y)$.

70um polystyrene sphere synchrotron imaged at different distances 50m from x-ray source



In-line phase-contrast: Lung aeration at birth



This phase-contrast work on lung aeration at birth in pre-term rabbit pups was used to investigate the benefits of positive end-expiratory pressure (PEEP) for mechanical ventilation of pre-term babies

Monash Physiology

Stuart Hooper

Megan Wallace

Melissa Siew

Monash Physics

Rob Lewis

Marcus Kitchen

Michael Morgan

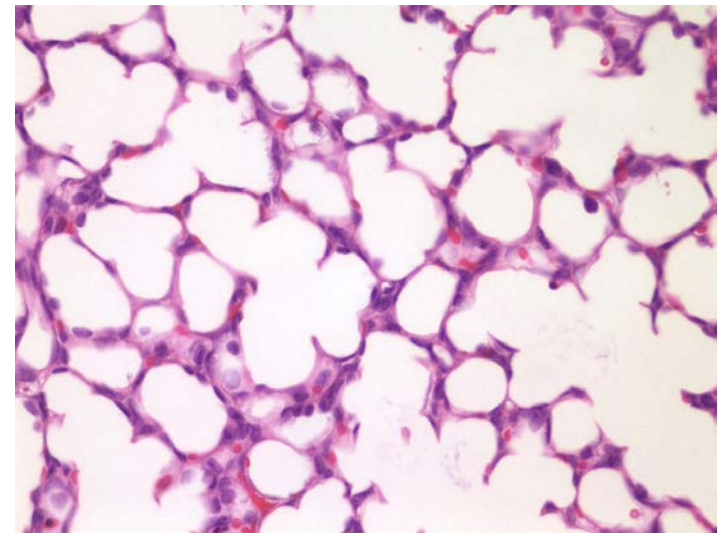
SPring-8

Naoto Yagi

Kentaro Uesugi

Funding by ARC, AMRFP

Lung structure of aerated lung goes from full of fluid in the womb to 80% air after normal birth



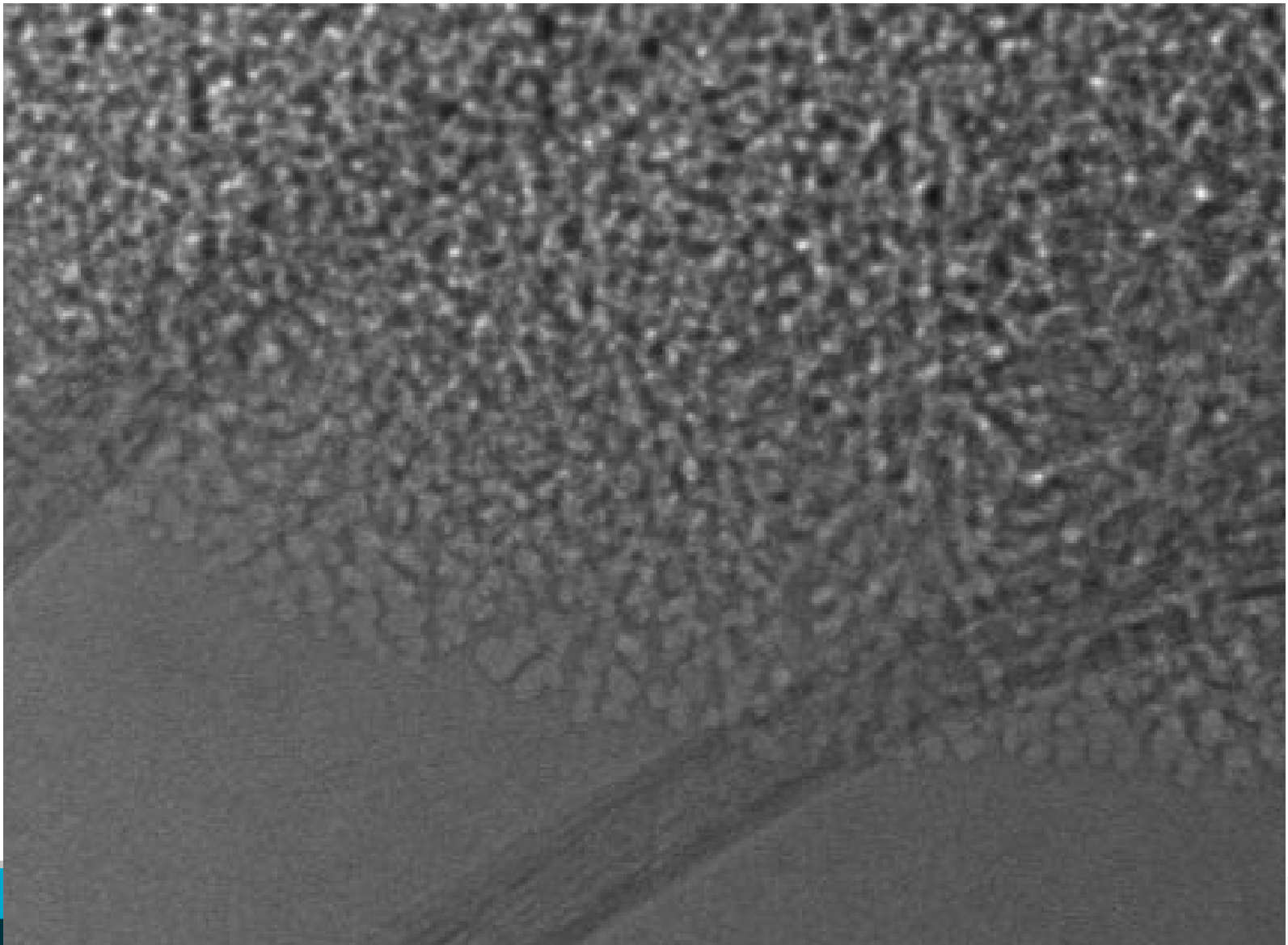
X-ray imaging of the lung

Absorption contrast

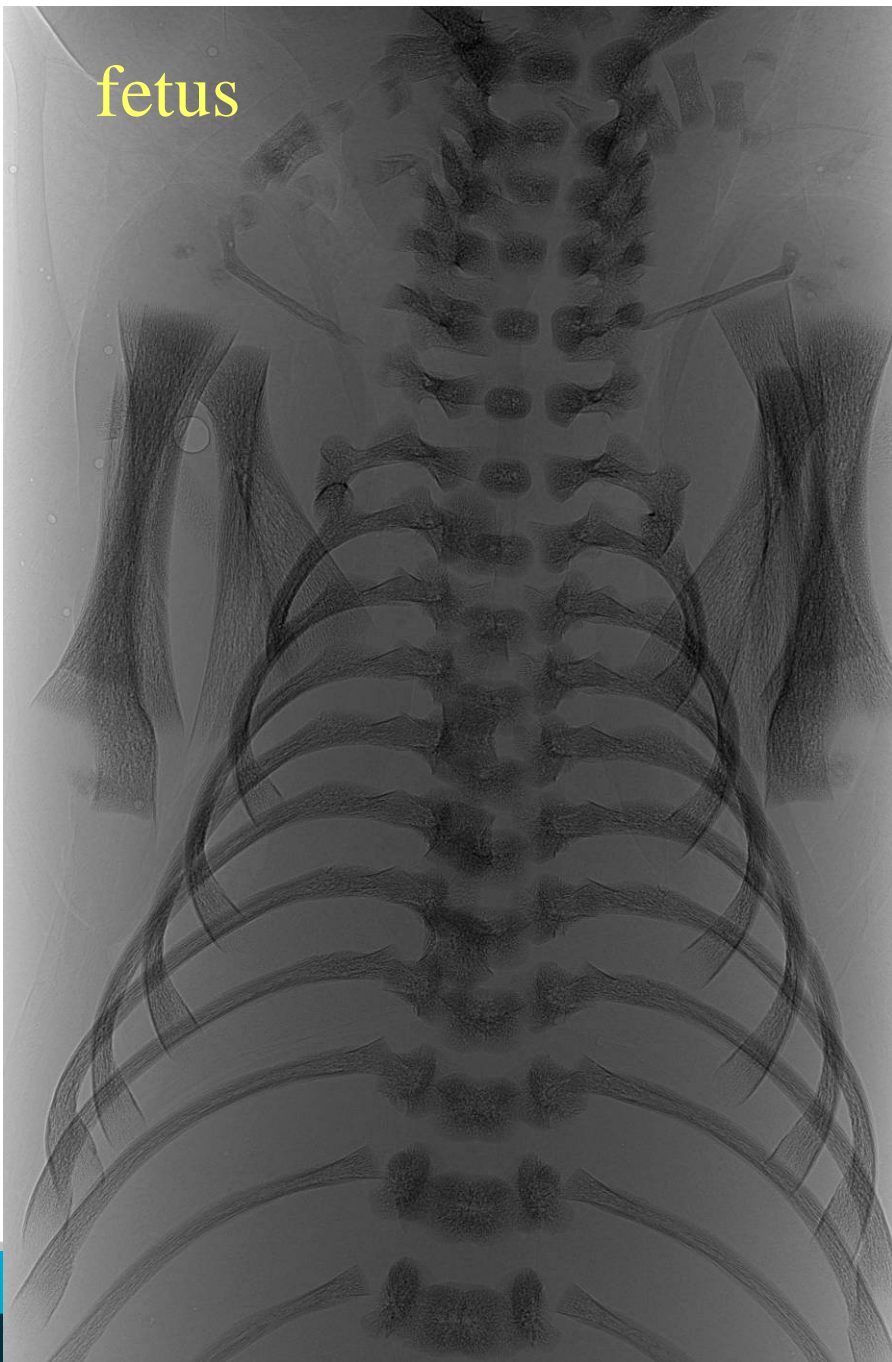


Phase contrast

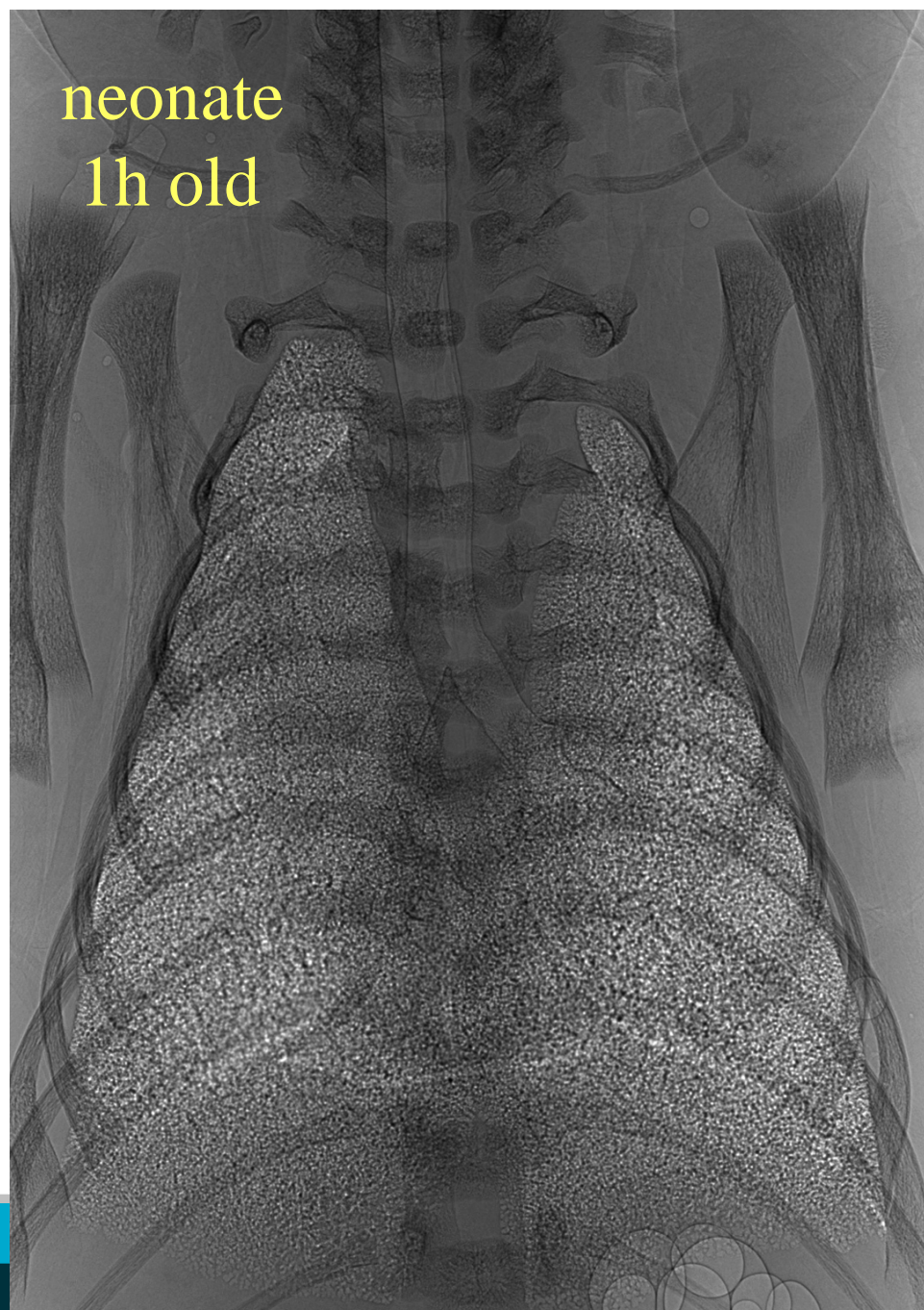




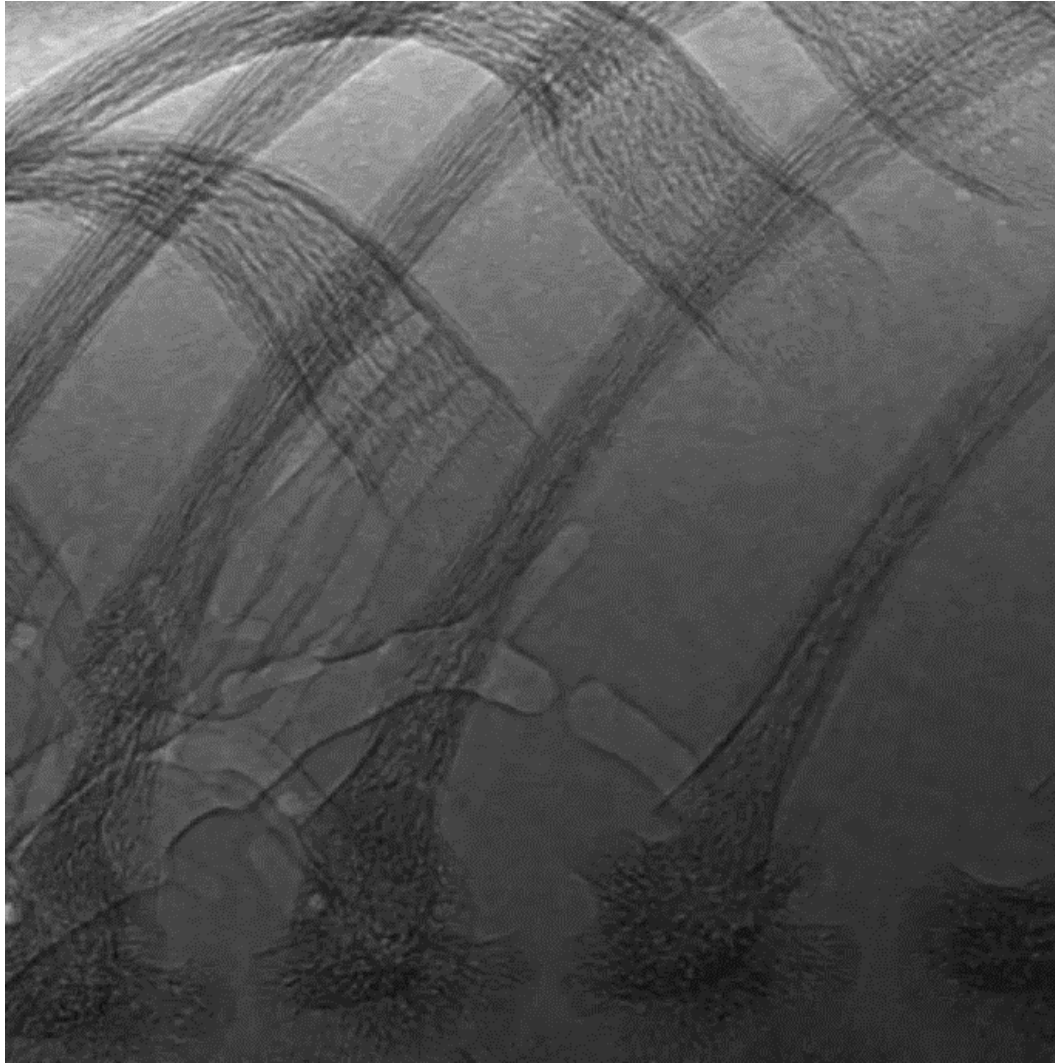
fetus



neonate
1h old



Lung aeration in a neonate rabbit pup



Ventilation comparison with/without PEEP

No PEEP – airways collapse back after deflation



PEEP – airways remain inflated promoting fluid clearance



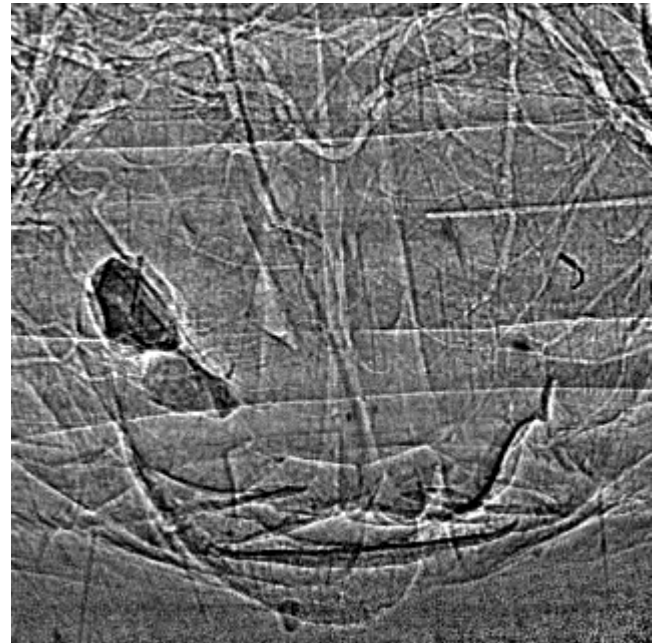
In-line phase-contrast: Bombardier beetle

Bombardier beetle (Brachinini) has unusual defence mechanism – jet of scalding defensive irritant spray.

Arndt and colleagues used high-speed x-ray phase-contrast imaging at APS of the beetles spraying fluid to see what was happening inside and learn about mechanism.



Movie acquired at 2000fps
slowed down to 80x to 25fps



Eric m. Arndt, Wendy Moore, Wah-Keat Lee, Christine Ortiz,
Science, 01 may 2015 : 563-567, 2015

Mechanism revealed

The upper (blue) chamber contains a solution of hydrogen-peroxide and hydroquinones. The lower chamber is connected to the outside and contains enzymes. A droplet or the fluid from the upper chamber is squirted through a fast moving valve into the lower chamber, where it reacts violently, liberating oxygen, heat and water and other products which are directed into a high-speed jet by the rigid chamber structure. This happens in a series of rapid pulses lasting a few ms.

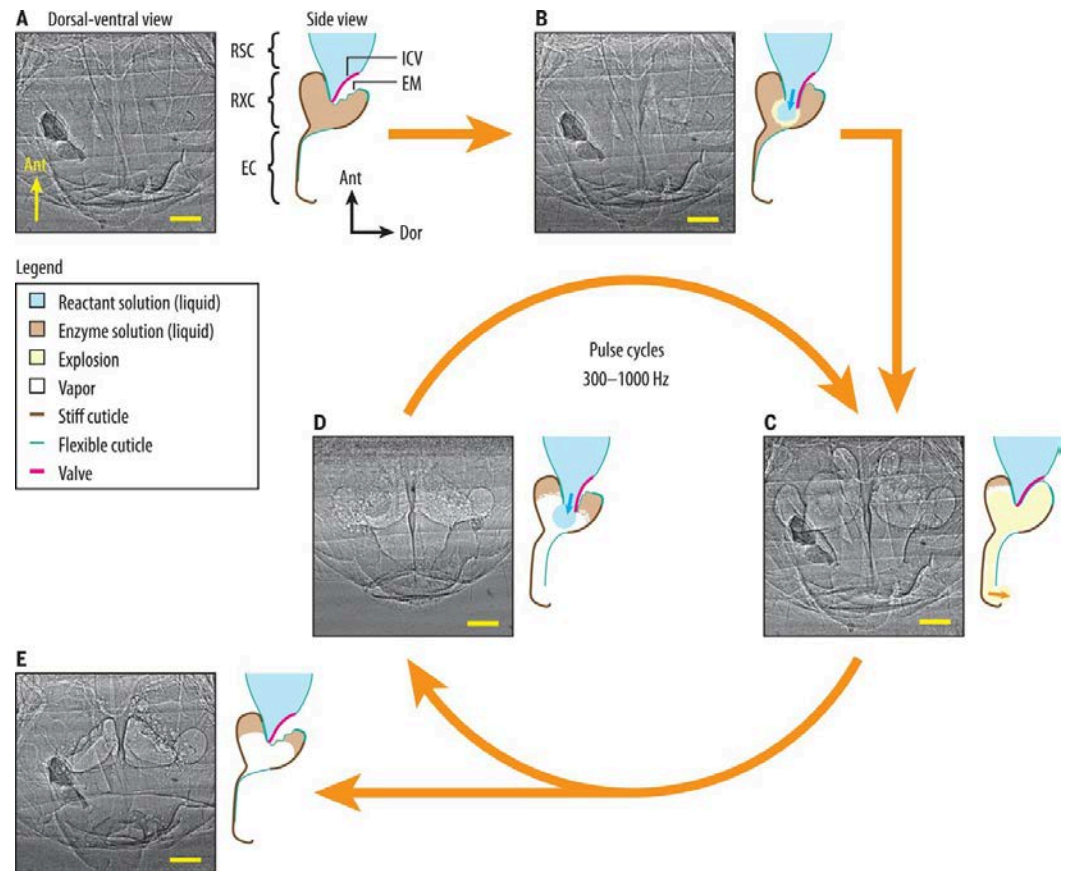


Fig 3 from: Eric m. Arndt, Wendy Moore, Wah-Keat Lee, Christine Ortiz, *Science*, 01 may 2015 : 563-567, 2015

Quantitative data from in-line phase-contrast

In-line phase contrast data is typically a mix of absorption contrast and edge-enhanced phase-contrast corresponding to the second derivative of the phase shift distribution of the images object. Unlike absorption contrast data the intensity no longer has a simple relationship with the thickness of the sample.

For a homogenous material, information about the thickness of the object can be obtained from a single image using **phase-retrieval**.

A commonly used algorithm in this case is that of Paganin et al ([J Microsc.](#) 2002 Apr;206(Pt 1):33-40). This is effectively a specialised low pass Fourier filter similar to an inverse Laplacian. This has been implemented in the following software packages: X-TRACT, AnkaPhase, STP and TomoPy. Even for non-homogenous materials, performing phase-retrieval is very useful for phase-contrast tomography.

For homogenous medium of thickness t

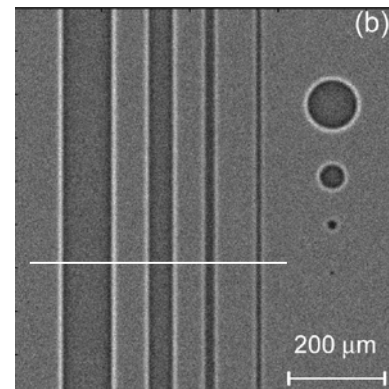
Phase shift

$$\phi = \psi t$$

Attenuation

$$I/I_0 = e^{-\mu t}$$

Solve for t (single variable)

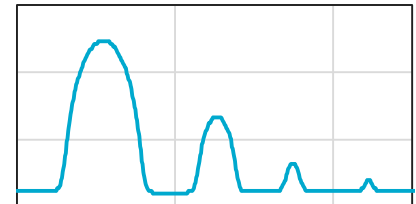
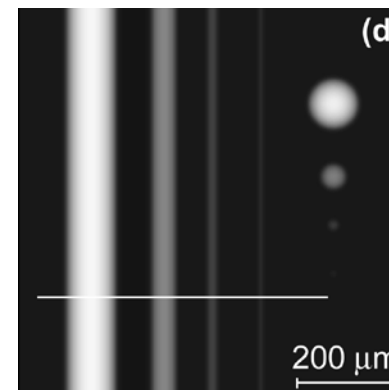


From: Anna Burvall, et al, Opt. Express 19, 10359-10376 (2011)

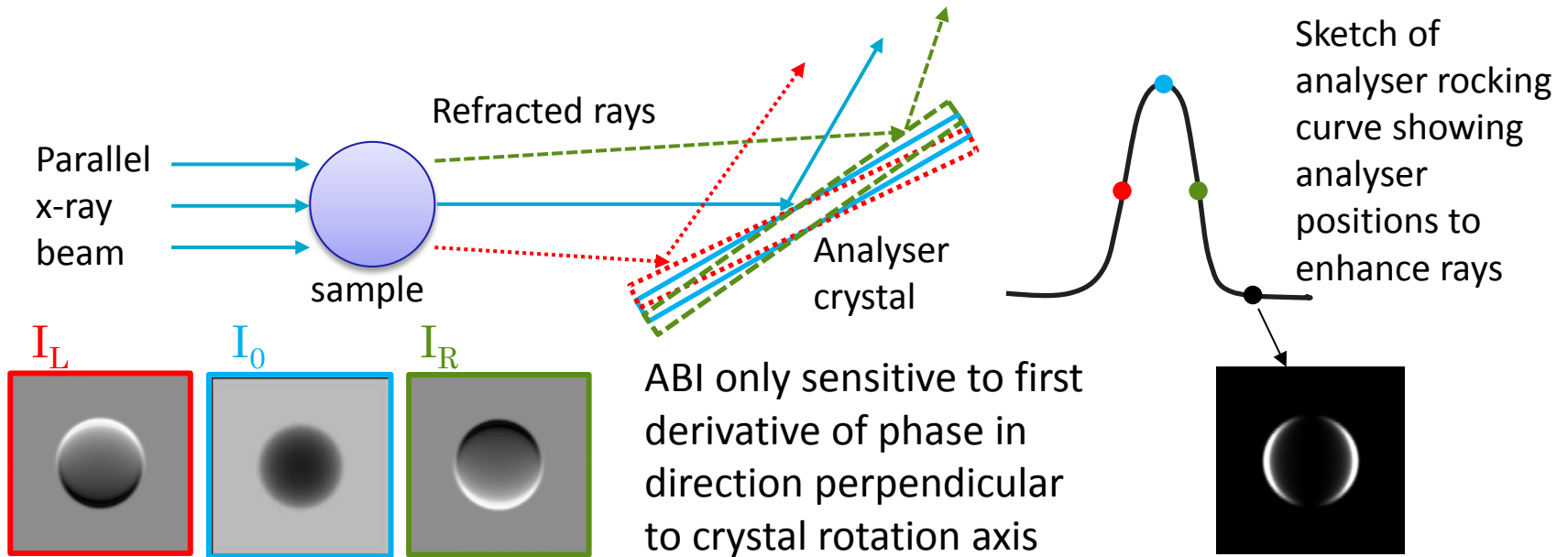
Synthetic inline phase-contrast image

Phase retrieved thickness map

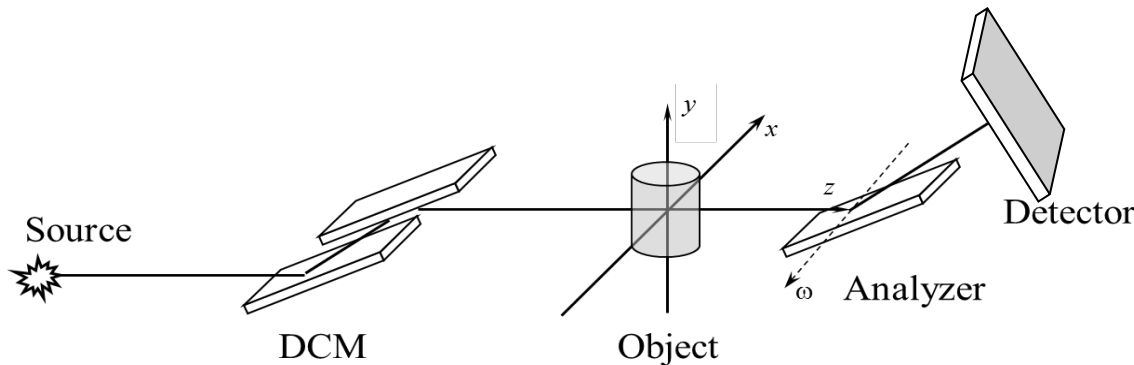
Line profiles through images



Analyser-based phase-contrast (ABI)

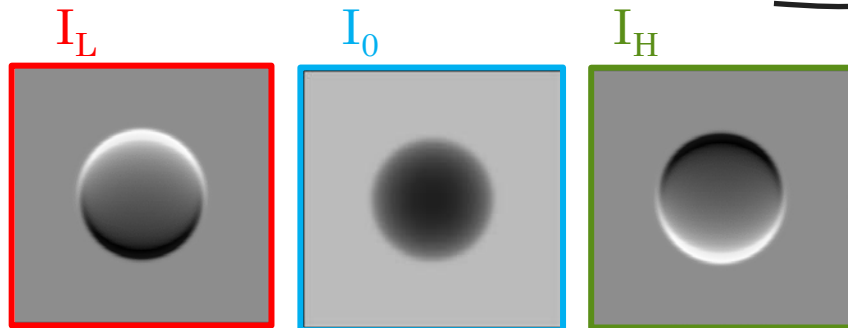


Dark field image is sensitive to scattered x-rays



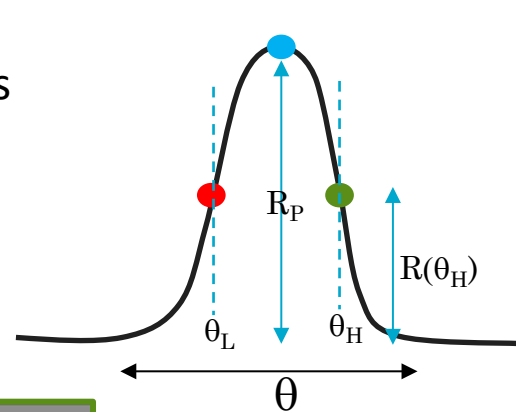
Analyser-based phase-contrast (ABI)

The refraction image (map of $\Delta\theta$) is calculated from the normalised difference of the images acquired on either side of the rocking curve

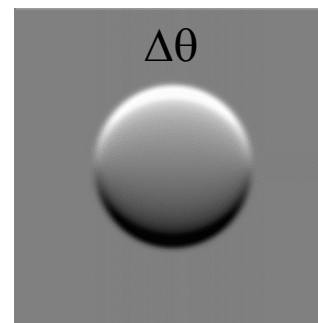
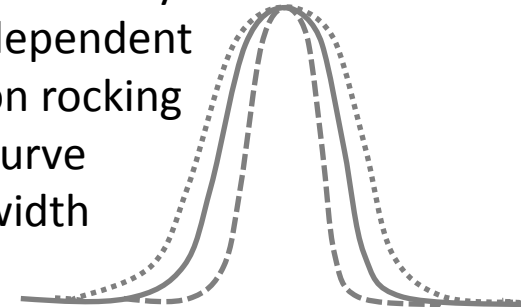


$$\Delta\theta_z = \frac{I_H R(\theta_L) - I_L R(\theta_H)}{I_L (dR/d\theta)_{(\theta_H)} - I_H (dR/d\theta)_{(\theta_L)}}$$

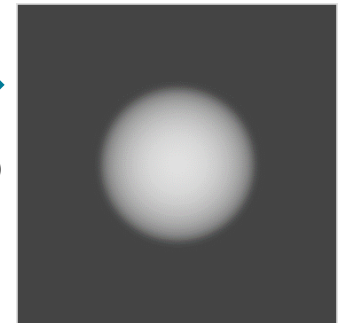
$$\Delta\theta_z = \frac{-R_p}{2(dR/d\theta)_{(-w/2)}} \frac{I_H - I_L}{I_H + I_L}$$



Sensitivity dependent on rocking curve width



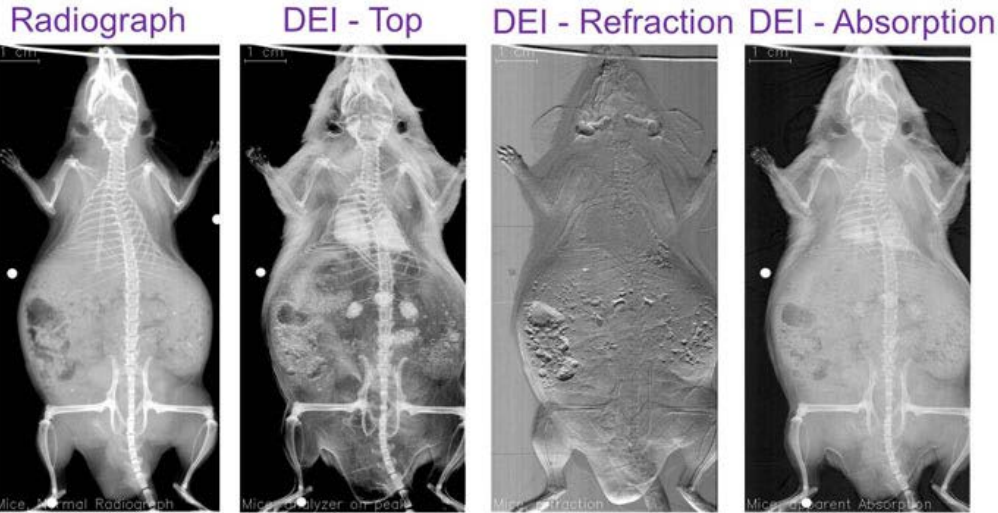
Integrate to obtain phase-map



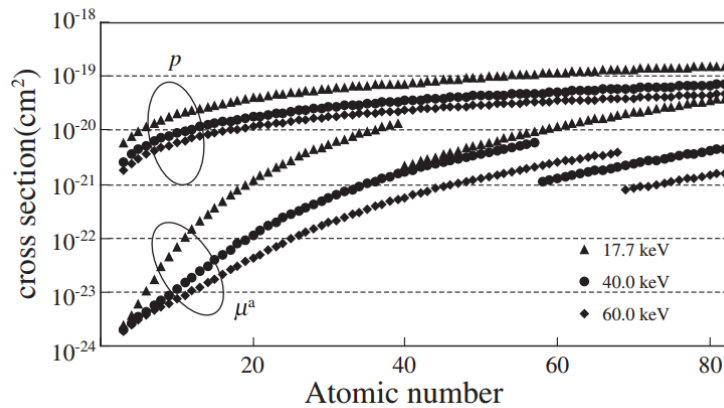
For symmetric positions at half-max

$$I_R = \frac{I_H + I_L}{2R_p}$$

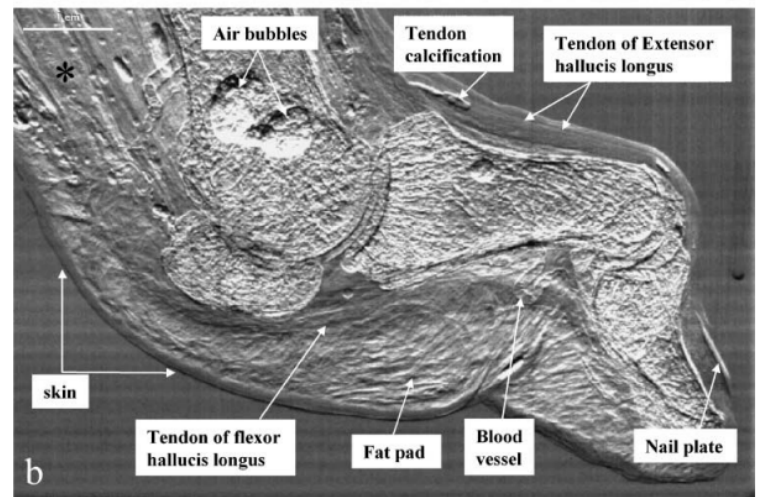
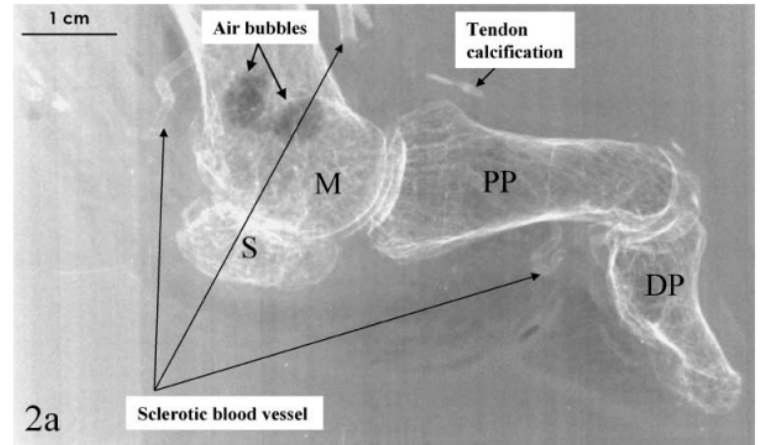
Analyser-based imaging from NSLS



Data from NSLS X15-A



Momose, Jpn. J. Appl. Phys., Vol. 44, No. 9A, 2005



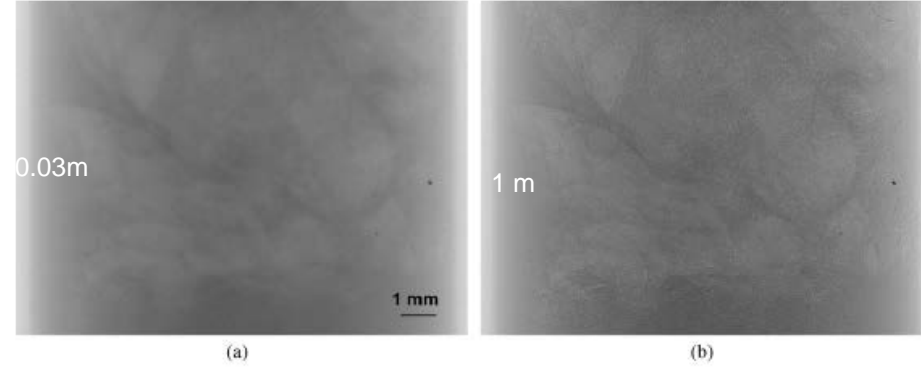
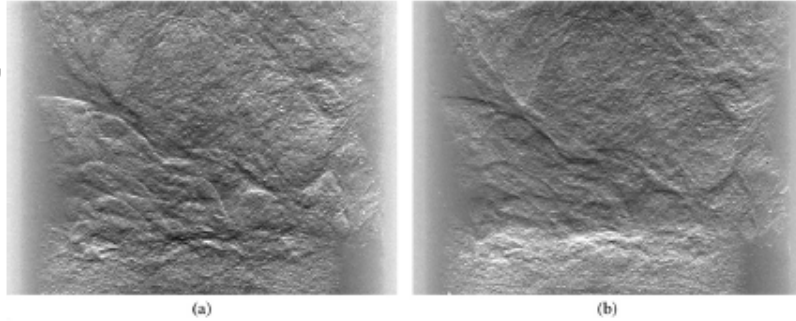
Jun Li, Zhong Zhong et al J. Anat. (2003) 202, pp463–470

Comparison of ABI and in-line PCI

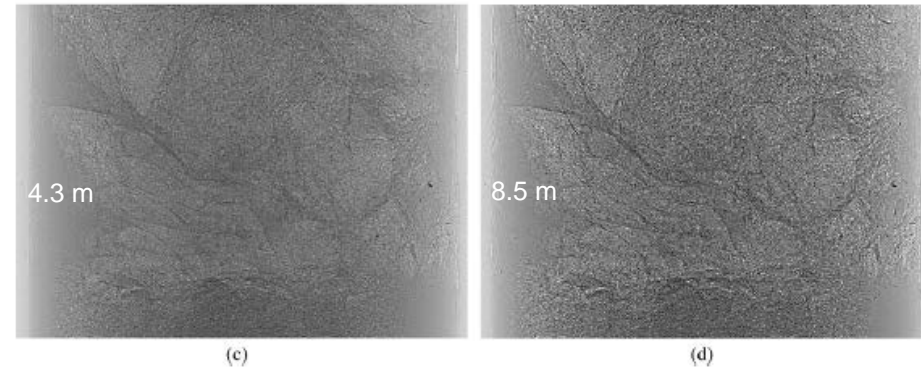
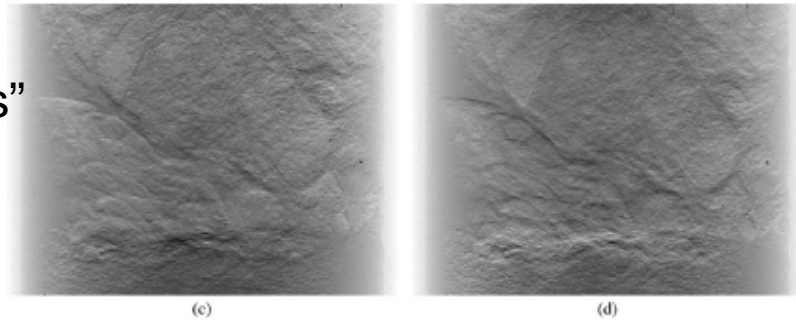
Analyser-based

In-line phase-contrast

“tails”



“flanks”



“peak”

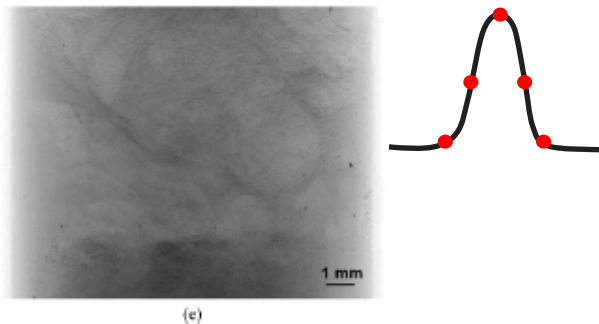
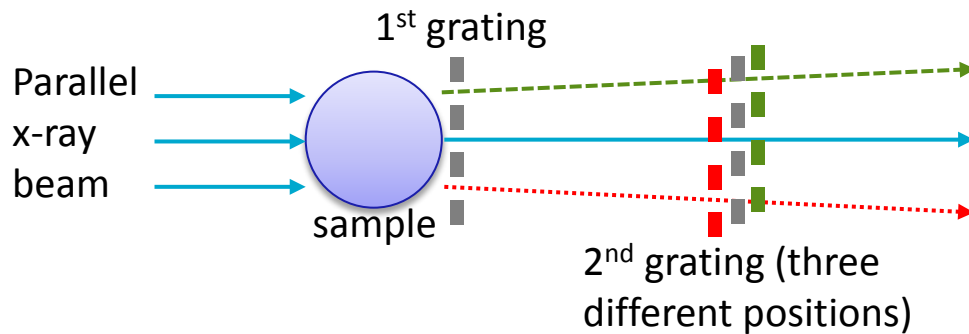


Figure 12. PPI images of the 13 mm diameter biopsy sample at an x-ray energy of 25 keV. (a)–(d) were acquired at 0.03 m, 1 m, 4.3 m and 8.8 m, respectively.

E Pagot et al Phys. Med. Biol. 50 (2005) 709–724

Grating-based imaging

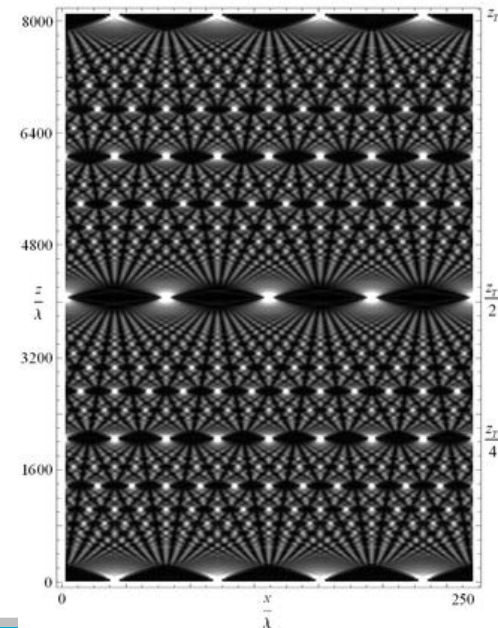


Different grating positions transmit and block beams refracted in different directions (shown as red, blue and green)

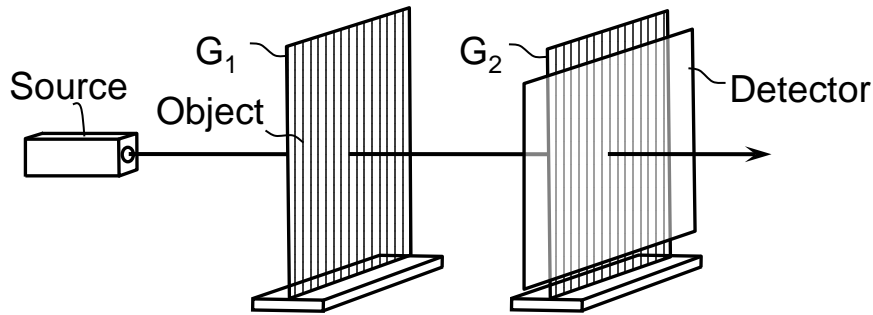
Due to the Talbot effect, the first grating produces interference patterns in the beam as it propagates. A 'self-image' pattern of the grating occurs at distances corresponding to multiples of the Talbot distance. The second grating is placed at one of these locations.

The pitch of the grating is small compared to the detector pixel size so the detector does not resolve fringes but detects transmitted intensity.

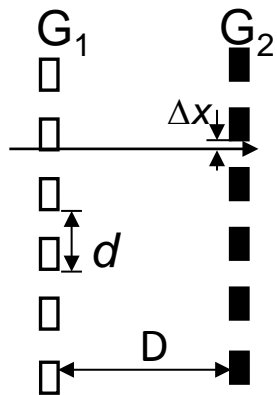
In grating-based phase-contrast a grating immediately next to the sample splits the beam into narrow beams. A second aligned grating can detect deflection of the beam by moving horizontally with respect to the first grating and measuring the change in transmitted intensity



Grating-based imaging



The intensity on the detector is recorded for difference values of Δx as the 2nd grating is moved over a total of one grating period. This is equivalent to ABI measurements taken at different points on the rocking curve.



Critical grating parameters for a typical set up are grating separation (D), grating period (d) and relative displacement (Δx)

Weitkamp et al, Optics Express Vol. 13, Issue 16, 6296 (2005)

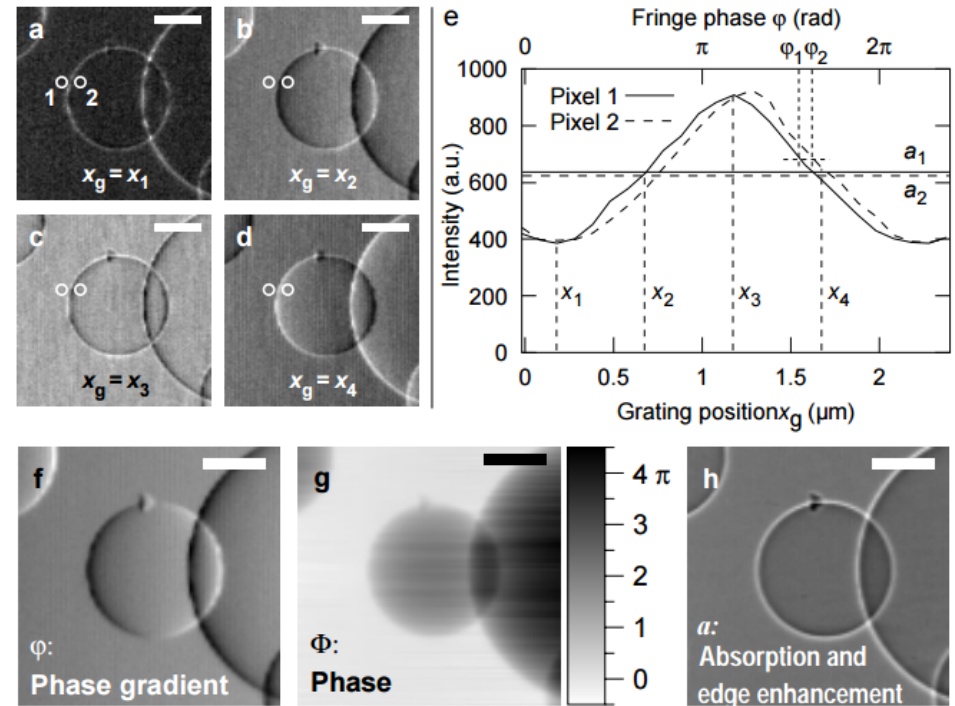
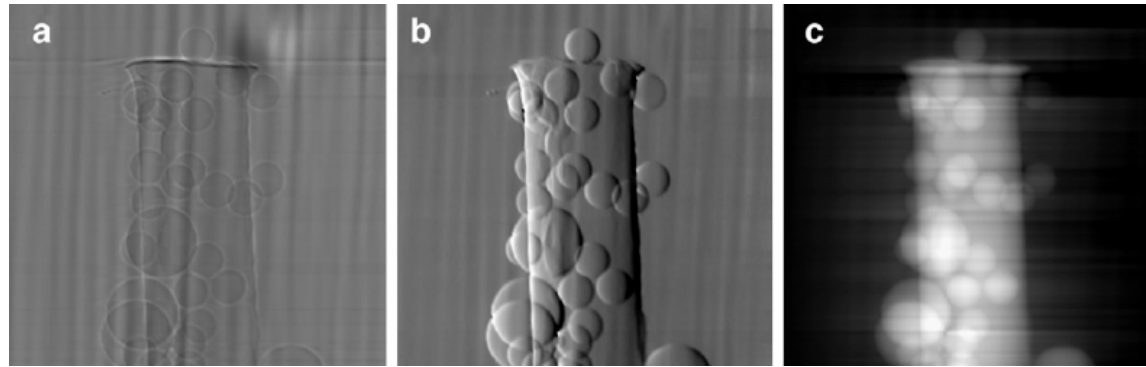


Fig. 2. Principle of phase stepping. (a-d) Interferograms of polystyrene spheres (100 and 200 μm diameter), taken at the different relative positions $x_g = x_1, \dots, x_4$ of the two interferometer gratings. (e) Intensity oscillation in two different detector pixels $i = 1, 2$ as a function of x_g . For each pixel, the oscillation phase ϕ_i and the average intensity a_i over one grating period can be determined. (f) Image of the oscillation phase ϕ for all pixels. (g) Wave-front phase Φ retrieved from ϕ by integration. (h) Image of the averaged intensity a for all pixels, equivalent to a non-interferometric image. The length of the scale bar is 50 μm .

Grating-based imaging

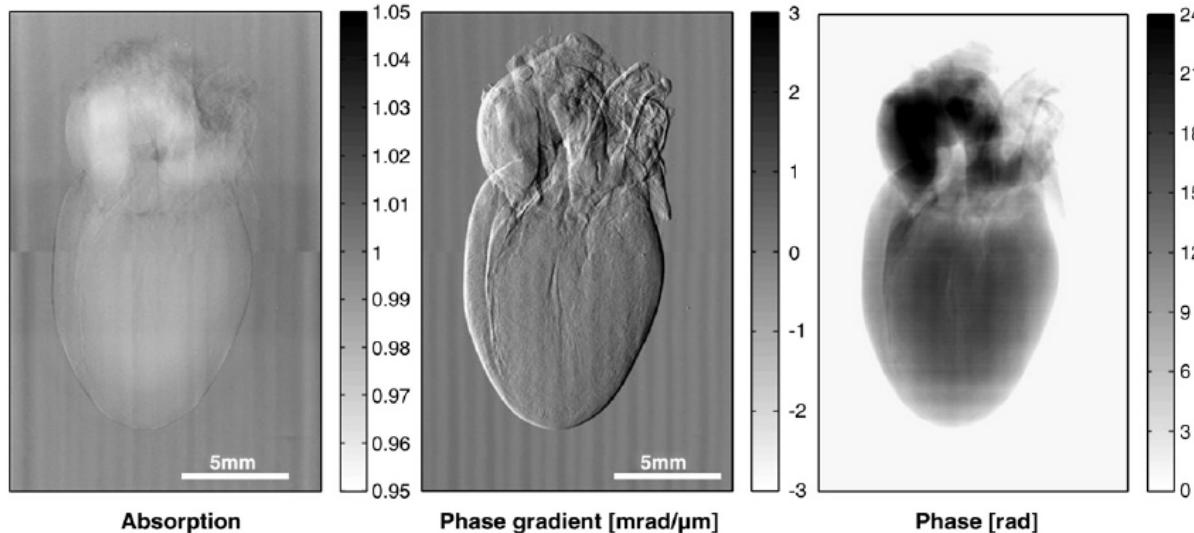
David et al Spectrochimica Acta Part B Atomic Spectroscopy 62(6), 2007



As with other phase-contrast techniques the grating based method is sensitive to low-Z materials and small phase shift.

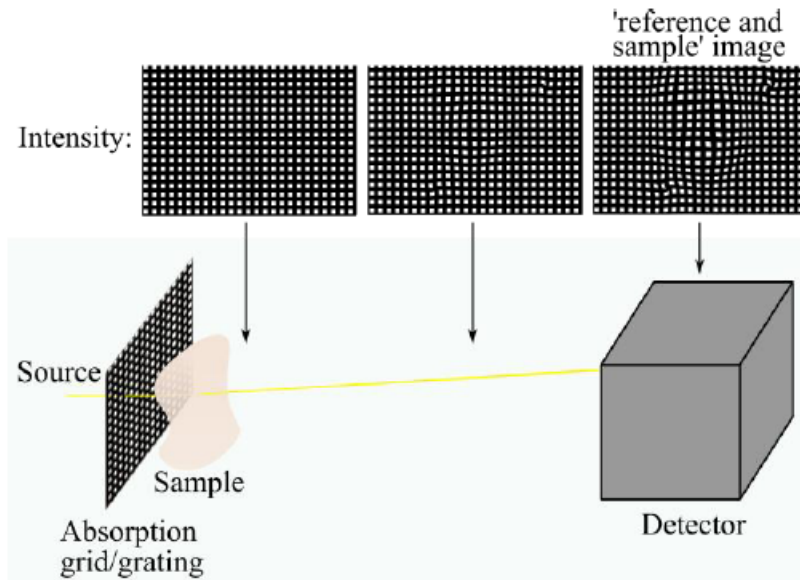
Imaging resolution is limited by the detector and by the grating period.

Increasing the grating gap increases phase sensitivity but decreases spatial resolution and may also decrease contrast for finite source size.



Single-shot grating method

Morgan KS, et al PLoS ONE 8(1): e55822



This method uses the distortion imposed by a sample on a patterned intensity distribution from a grid to determine the phase-shift.

The method used by Morgan et-al is similar in principle to a Shack-Hartmann interferometer. A reference image is acquired at the start with only the grid in place. An image is acquired with the grid plus the sample.

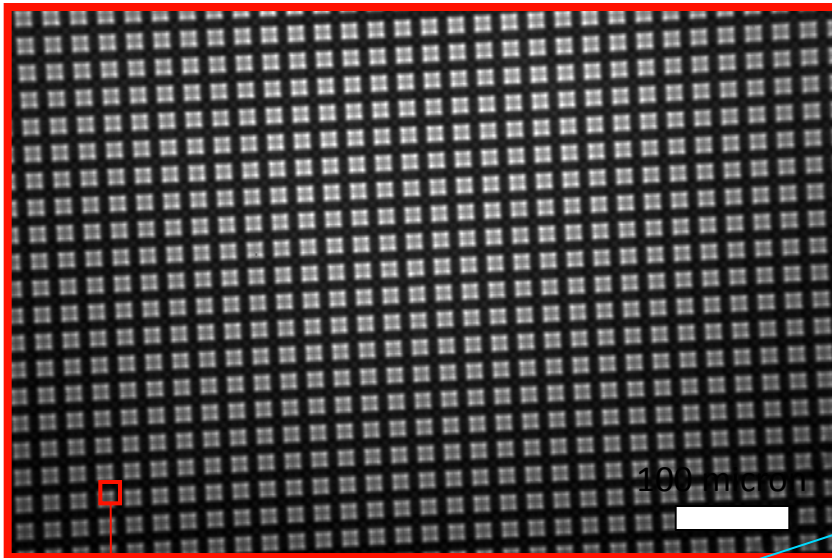
Local cross-correlation is used to determine the displacement of the grid features due to the phase shift imposed by the sample. From this the phase-map can be extracted. A similar one-shot method using Moire fringes has been demonstrated by Momose, using Fourier methods to extract the phase.

Advantages: sensitive to phase in both X and Y direction; single-shot for dynamic systems

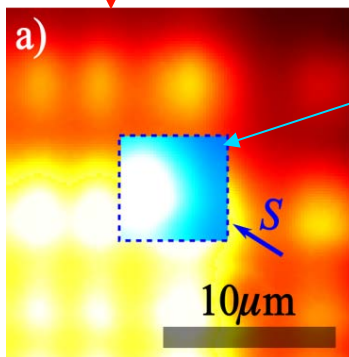
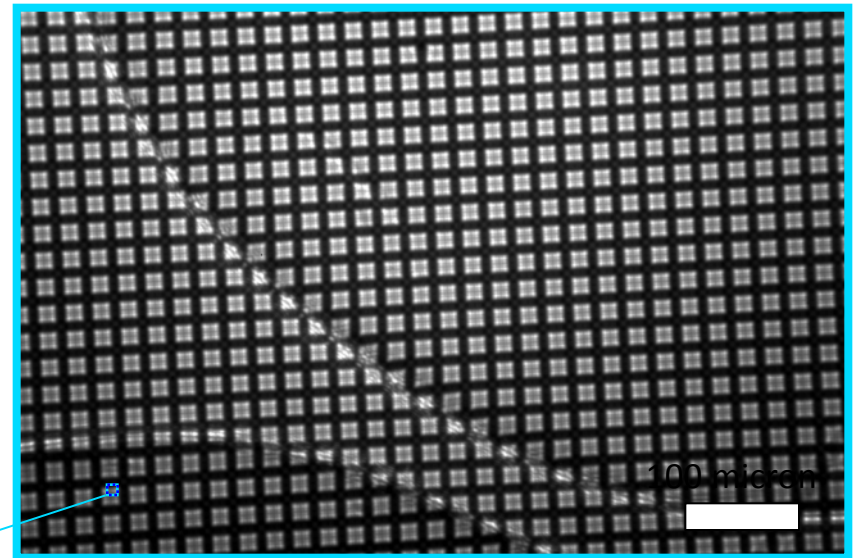
Disadvantage: Resolution limited by grid features used for analysis (significantly lower than resolution of detector)

Recovering the shift in reference pattern

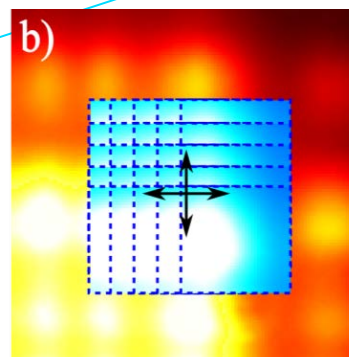
2D grid only image:



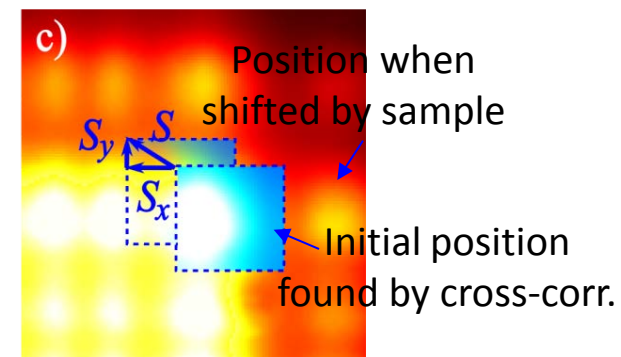
2D grid and sample image:



Take interrogation window from grid & sample image



Find initial position by cross-correlation with grid image



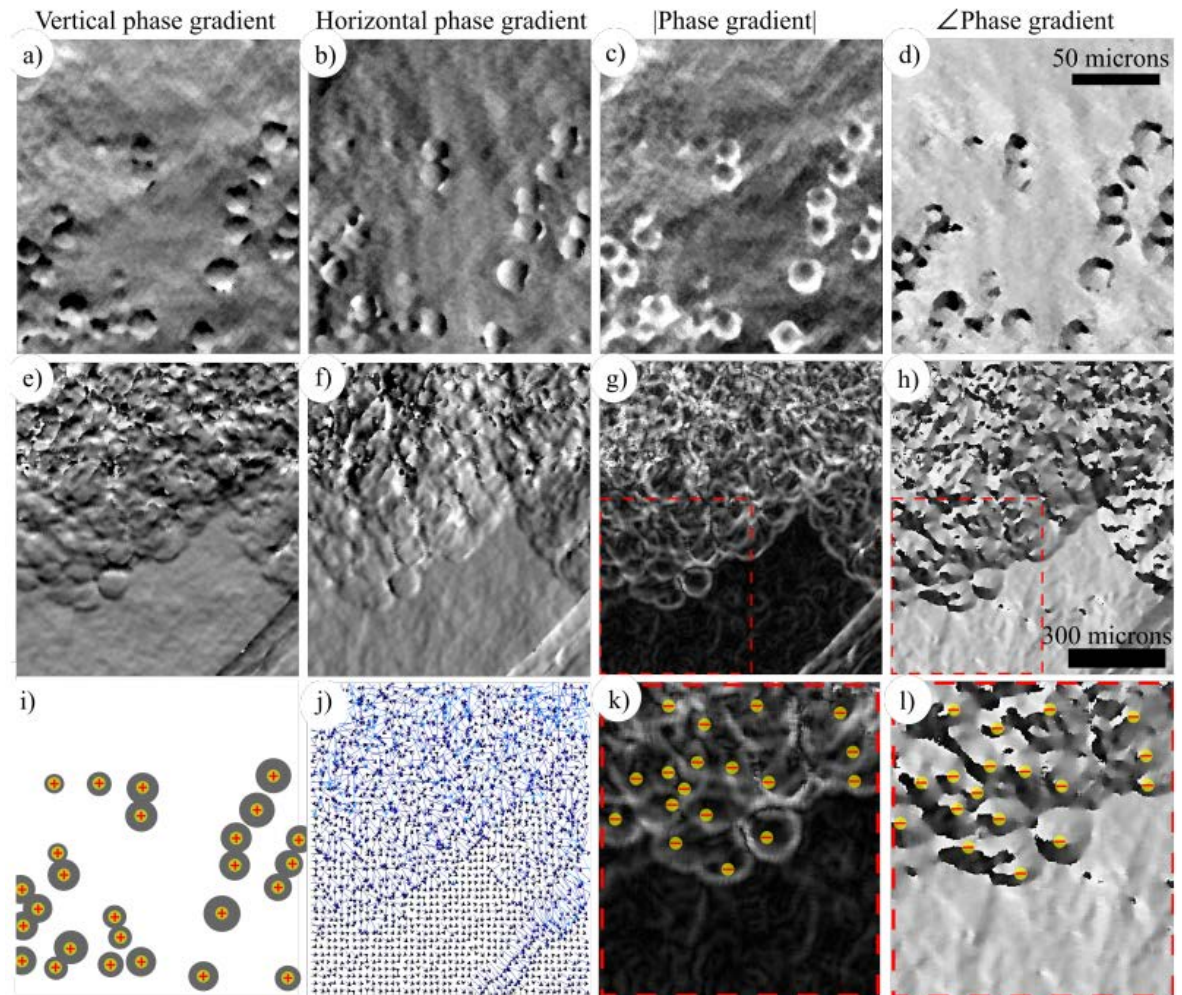
Resolve the shift S incurred by the sample into S_x and S_y

Phase measurement in two dimensions

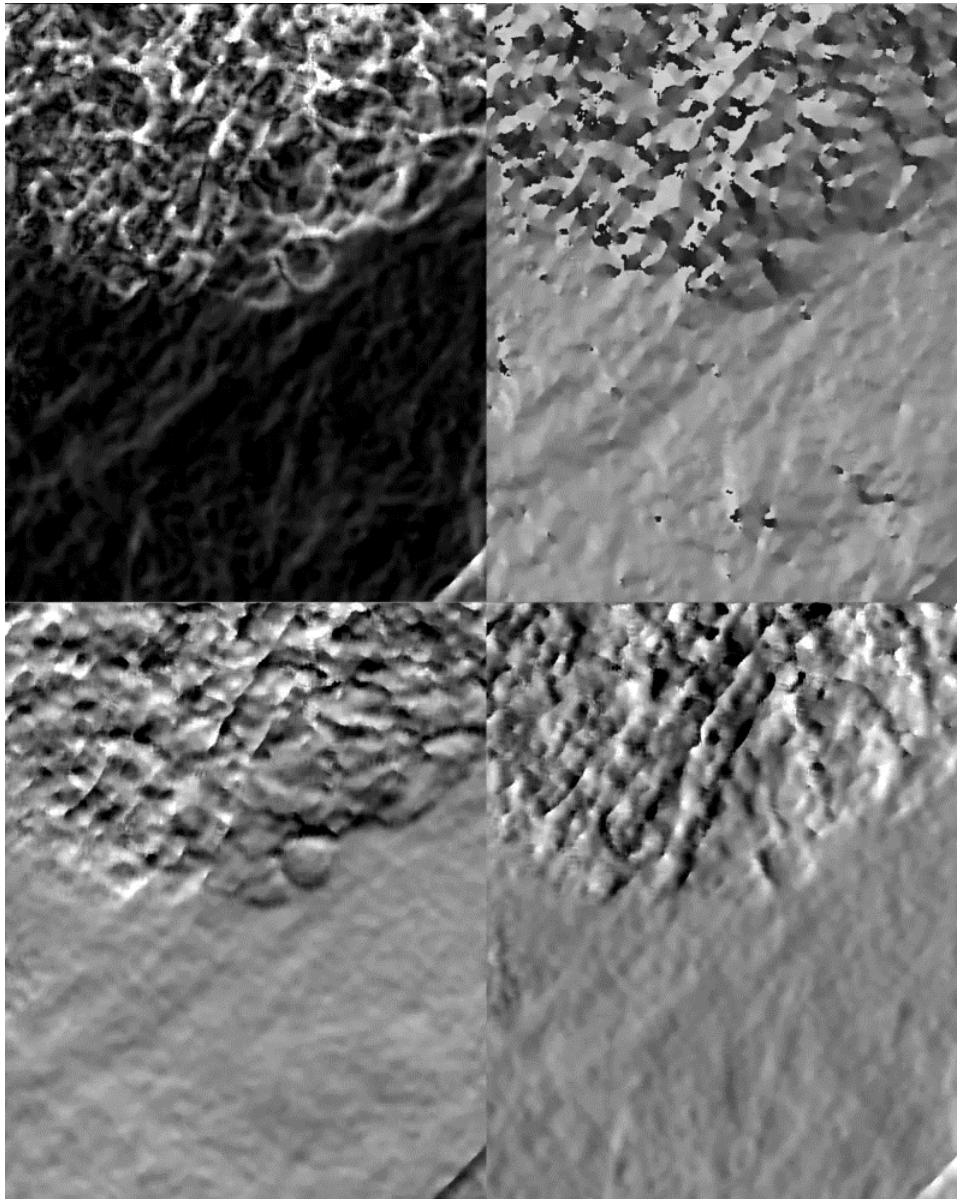
Glass beads transiting mouse airway surface

Lower periphery of inflated mouse lung

Local phase maxima of beads, phase-gradient vector map of lung and local phase-minima in phase gradient and angle for lung



Morgan et al, Optics Express (2016) Vol. 24, No. 21, 24436



The lower periphery of a mouse lung during two breaths, using single-grid x-ray phase imaging to extract a) magnitude and b) angle of the phase gradient, and c) vertical and d) horizontal phase gradients.

Data acquired Spring 8

Morgan et al, Optics Express (2016) Vol. 24, No. 21, 24436

Thank you

CSIRO Manufacturing
Sheridan Mayo

t +61 2 96185944

e sherry.mayo@csiro.au

CSIRO MANUFACTURING
www.csiro.au

